

**Intramolecular Charge Transfer with Crystal Violet Lactone in
Acetonitrile as a Function of Temperature.
Reaction is Not Solvent-Controlled**

Sergey I. DRUZHININ,^{*,a} Attila DEMETER,^b Klaas A. ZACHARIASSE,^{*,a}

^aMax-Planck-Institut für biophysikalische Chemie, Spektroskopie und Photochemische Kinetik,
37070 Göttingen, Germany

^bInstitute of Materials and Environmental Chemistry, Research Centre for Natural Sciences,
Hungarian Academy of Sciences, 1025 Budapest, Pusztaszeri u. 59-67, Hungary

Abstract

Intramolecular charge transfer (ICT) with crystal violet lactone (CVL) in the excited singlet state takes place in solvents more polar than *n*-hexane, such as ethyl acetate, tetrahydrofuran, and acetonitrile (MeCN). In these solvents, the fluorescence spectrum of CVL consists of two emission bands, from a locally excited (LE) and an ICT state. The dominant deactivation channel of the lowest excited singlet state is internal conversion, as the quantum yields of fluorescence (0.007) and intersystem crossing (0.015) in MeCN at 25 °C are very small. CVL is a weakly-coupled electron donor/acceptor (D/A) molecule, similar to an exciplex $^1(A\cdot D^+)$. A solvatochromic treatment of the LE and ICT emission maxima results in the dipole moments $\mu_e(\text{LE}) = 17$ D and $\mu_e(\text{ICT}) = 33$ D, much larger than those previously reported. This discrepancy is attributed to different Onsager radii and spectral fluorimeter calibration. The LE and ICT fluorescence decays of CVL in MeCN are double exponential. As determined by global analysis, the LE and ICT decays at 25 °C have the times $\tau_2 = 9.2$ ps and $\tau_1 = 1180$ ps, with an amplitude ratio of 35.3 for LE. From these parameters, the rate constants $k_a = 106 \times 10^9 \text{ s}^{-1}$ and $k_d = 3.0 \times 10^9 \text{ s}^{-1}$ of the forward and backward reaction in the $\text{LE} \rightleftharpoons \text{ICT}$ equilibrium are calculated, resulting in a free enthalpy difference ΔG of -8.9 kJ/mol. The amplitude ratio of the ICT fluorescence decay equals -1.0, which signifies that the ICT state is not prepared by light absorption in the S_0 ground state, but originates exclusively from the directly excited LE precursor. From the temperature dependence of the fluorescence decays of CVL in MeCN (-45 to 75 °C), activation energies $E_a = 3.9$ kJ/mol ($\text{LE} \rightarrow \text{ICT}$) and $E_d = 23.6$ kJ/mol ($\text{ICT} \rightarrow \text{LE}$) are obtained, giving an enthalpy difference $\Delta H (= E_a - E_d)$ of -19.7 kJ/mol, and an entropy difference $\Delta S = -35.5$ J/Kmol. These data show that the ICT reaction of CVL in MeCN is not barrierless. The ICT reaction time of 9.2 ps is much longer than the mean solvent relaxation time of MeCN (0.26 ps), indicating, in contrast with earlier reports in the literature, that the reaction is not solvent controlled. This conclusion is supported by the observation of double exponential LE and ICT fluorescence with the same decay times.

Keywords: fluorescence, dual emission, electron donor/acceptor, solvent relaxation, solvatochromy, decays

Introduction

Crystal violet lactone (CVL) consists of a 6-dimethylaminophthalide (6DMAPd) unit and two *N,N*-dimethylaniline (DMA) subgroups, connected by a tetrahedral spiro carbon atom, which is part of 6DMAPd. This C atom is the center of three C-C bonds and one C-O bond. The two DMAs are not in an exactly orthogonal configuration relative to 6DMAPd. In the CVL crystal,^{1,2} the planar aminophthalide makes different dihedral angles with the two DMA planes, 60.9° and 87.4°, whereas these subgroups are themselves at a dihedral angle of 69.0°.¹ Consequently, the angles around the spiro carbon of CVL deviate somewhat from the ideal tetrahedral angle of 109.5° for a pure sp³ carbon: between 101.8 and 111.4°, the two limiting angles involving the oxygen atom of the lactone ring.¹ The lengths of the bonds connecting the spiro C atom to the C neighbours are approximately equal (151.4 to 151.8 pm), practically the same as the C-C bond length of 152 pm in *n*-alkanes.³ Also, the bond between the spiro C and the lactone O (149.1 pm) is much longer than the O-C(=O) bond of 135.5 pm, which shows that the delocalization of the electrons in the aromatic ring of the DMAs does not extend to the central carbon atom.^{1,2} These data¹ thus indicate that for CVL in the ground state *S*₀, the electronic coupling between the two DMAs and 6DMAPd is very small. The observation that the absorption spectrum of CVL in acetonitrile (MeCN) is a superposition of those² of DMA and 6DMAPd verifies that the electron donor and acceptor subgroups are indeed only weakly conjugated in *S*₀.

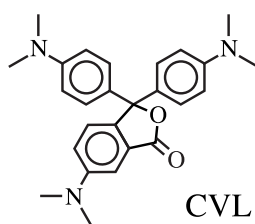


Chart 1

Research on fluorescence, charge transfer or excited states of CVL appeared in the literature rather long after the first publication in 1947, a patent describing the role of CVL as a key component in pressure-sensitive and thermographic recording material ('carbonless' copy paper).^{4,2} This initial absence of investigations in the excited state is obviously due to the fact that the thermographic process, the conversion to the crystal violet cation upon dissociation of the C-O bond in the lactone ring in the presence of a proton donor, occurs in the ground state *S*₀.

In the first study of the photochemistry of CVL, attention was paid to fluorescence quenching

and the formation of a triphenyl methyl cation.⁵ The fluorescence spectrum of CVL in MeCN with two emission bands (dual fluorescence, see below) was not further discussed. It was concluded that electron transfer takes place with CVL in MeCN, in competition with intersystem crossing (ISC). From the very small overall fluorescence quantum yield $\Phi(\text{flu}) = 1.3 \times 10^{-3}$, the ISC yield was assumed to be effectively equal to unity: $\Phi(\text{ISC}) \sim 1.0$, although experimental information to support this claim was not presented.⁵ It was thought to arise from a $n\pi^*$ admixture to the $\pi\pi^*$ lower excited singlet state because of the very small value of $\Phi(\text{flu})$. In the present contribution, triplet-triplet (TT) absorption measurements reveal that $\Phi(\text{ISC})$ of CVL in MeCN is in fact much smaller (0.015). By employing the Stern-Volmer quenching product $k_q \tau$, where k_q is the quenching rate constant (taken as $2 \times 10^{10} \text{ M}^{-1}\text{s}^{-1}$) and τ is the fluorescence lifetime, $\tau = 1.8 \text{ ns}$ was calculated for CVL in MeCN, at room temperature.⁵ The photophysics of CVL has been investigated in a series of aprotic solvents at 22 °C.² In protic solvents, efficient cation formation operates via photodissociation of the C-O bond in the lactone ring,⁵ which process does not occur in aprotic media.² In nonpolar or slightly polar solvents, from *n*-hexane ($\epsilon^{25} = 1.88$) to tetrahydrofuran (THF, $\epsilon^{25} = 7.39$), the fluorescence spectrum of CVL was reported to consist of a single emission band, similar to that of 6DMAPd.^{2,6} In the first excited singlet state S_1 of CVL in media such as *n*-hexane, the excitation is hence localized on the 6DMAPd unit. It is therefore termed here a locally excited (LE) state.⁷⁻¹⁰ The same nomenclature is used in refs 11-14.

In solvents more polar than THF, from 1,2-dichloroethane ($\epsilon^{25} = 10.4$) to strongly polar media such as MeCN ($\epsilon^{25} = 36.7$), an additional fluorescence band was observed to the red of the LE emission,⁶ originating from an intramolecular charge transfer (ICT) state, with a dipole moment $\mu_e(\text{ICT})$ of $\sim 25 \text{ D}$.² The shape of the ICT emission band of CVL was shown to be similar to that of malachite green lactone (MGL).^{2,15-19} Also the LE state was found to have a substantial dipole moment $\mu_e(\text{LE}) = 10.7 \text{ D}$, about the same as that of 6DMAPd (9.7 D), but much larger than the ground state dipole moment μ_g of 5.5 D.²

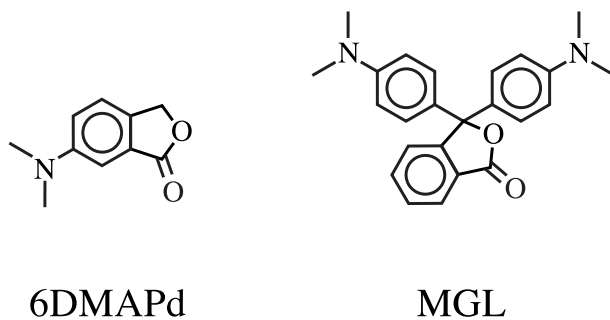


Chart 2

These data show that after excitation of CVL, an electron is transferred from either one of the two DMA moieties as the electron donor (D) to the 6DMAPd subunit as the electron acceptor (A). The resulting ICT state is considered to be an intramolecular exciplex,²⁰⁻²² consisting of D and A subgroups that only interact weakly. The dual (LE + ICT) fluorescence spectrum of CVL in MeCN is approximately the sum of the spectra of 6DMAPd (LE) and MGL (ICT). With MGL in MeCN, the LE \rightleftharpoons ICT equilibrium (with forward and backward rate constants k_a and k_d , Chart 3) is shifted far to the ICT side, which means that the LE emission is practically not visible in the overall photostationary fluorescence spectrum.¹⁵⁻¹⁹

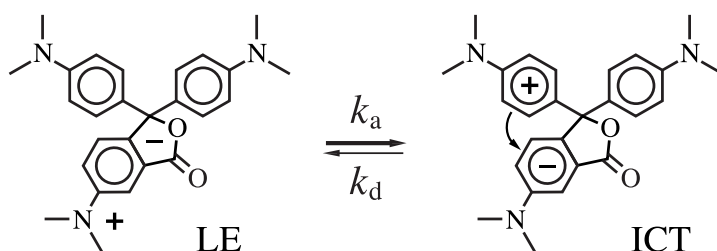


Chart 3

Transient absorption (TA) spectra of CVL have been measured with a temporal resolution better than 1 ns.² The TA spectrum in di-(*n*-butyl) ether (DBE, $\epsilon^{25} = 3.05$), contains a band with a maximum around 560 nm, similar to that of 6DMAPd, supporting the conclusion made on the basis of the LE fluorescence spectra as discussed above, that a LE \rightarrow ICT reaction does not occur in this weakly polar solvent. Also the TA decay time is equal to that of the LE fluorescence $\tau(\text{LE}) = 12.3$ ns in DBE. The TA spectrum directly after excitation of CVL in MeCN consists of two bands, one with relatively small intensity around 560 nm, similar to the LE absorption in DBE and a new stronger one peaking at ~ 470 nm, comparable to that of the radical cation of DMA.²³ This new band is hence attributed to the ICT state.

Later,²⁴ femtosecond TA spectra of CVL in three strongly polar media: MeCN ($\epsilon^{25} = 36.7$), dimethylsulfoxide (DMSO, $\epsilon^{25} = 46.5$), and propylene carbonate (PC, $\epsilon^{25} = 65.0$) at 22 °C were reported, with a time resolution better than 300 fs. For CVL in MeCN, TA spectra were measured over a time range from 0.5 to 30 ps. The double-peaked spectrum at 0.5 ps is similar to the LE TA spectrum of 6DMAPd. With time, the LE band with a maximum at ~ 517 nm decreases in intensity, accompanied by a simultaneous growing-in of the band (ICT) around 468 nm. In these spectra, an isosbestic point appears, showing the presence of at least²⁵ two excited states, in accordance with the two states (LE and ICT) in Scheme 1. The TA signal at 550 nm (LE) decays with a time τ_2 of 7.8 ps, whereas that at 470 nm (ICT) shows a growing-in with τ_2

= 9.5 ps. For CVL in PC, the TA spectra between 0.5 and 50 ps are similar to those in MeCN, likewise with an isosbestic point.²⁴ The observation that there is no or little time-development of the spectral position of the two bands of CVL in MeCN as well as PC, indicates that the dynamics of solvent relaxation is faster than the reaction time of the LE \rightarrow ICT reaction and that hence a dynamic fluorescence Stokes shift is absent, as will be further discussed below.

The TA spectrum of the LE band in PC around 580 nm shows a decay ($\tau_2 = 23$ ps), with a corresponding rise ($\tau_2 = 34$ ps) of the ICT TA band at 470 nm. In DMSO, the rise and decay times τ_2 are 15 ps (LE) and 12 ps (ICT). In these solvents, as well as in MeCN, the times $\tau_2(\text{LE})$ and $\tau_2(\text{ICT})$ are taken to be the same, within the experimental accuracy, with a mean time $\langle \tau_2 \rangle$ of 9 ps in MeCN, 14 ps in DMSO, and 29 ps in PC.²⁴

Because the intrinsic electron transfer time of the LE \rightarrow ICT reaction of CVL was considered to be ultrafast, similar to the ~ 100 fs determined for the structurally closely related MGL,¹⁵ the observed differences in the ICT reaction time τ_2 were attributed to the different solvent relaxation dynamics of MeCN, DMSO, and PC.²⁴ This interpretation is based on the mean solvent relaxation times $\langle \tau_{\text{sr}} \rangle$, 0.26 ps for MeCN (longest time $\tau_{\text{sr}}(\text{l}) = 0.63$ ps), 2.0 ps for DMSO (longest time 10.7 ps), and 2.0 ps for PC (longest time 6.57 ps).^{26,27} These times $\langle \tau_{\text{sr}} \rangle$ show a correlation with the solvent viscosity: $\eta^{25} = 0.343$ cP (MeCN), $\eta^{25} = 2.00$ cP (DMSO), and $\eta^{25} = 2.51$ cP (PC), with a 5.8 fold (DMSO) and a 7.3 fold viscosity increase relative to MeCN. Note, however, that the measured ICT reaction times $\tau_2(\text{ICT})$ of CVL, 9.5 ps (MeCN); 12 ps (DMSO), and 34 ps (PC),²⁴ are much longer than the corresponding $\langle \tau_{\text{sr}} \rangle$ of 0.26, 2.0, and 2.0 ps, by a factor of 37, 6, and 17, respectively. As compared with the longest time $\tau_{\text{sr}}(\text{l})$, the ratios $\tau_{\text{sr}}(\text{l})/\tau_2$ are smaller: 15, 1.1, and 5.2.

Solute Versus Solvent Relaxation Dynamics for CVL. It should be realized, in this connection, that contribution of low-amplitude but activated structural changes (bond lengths and angles) to the differences in $\tau_2(\text{ICT})$ of CVL in the various solvents cannot be a priori rejected. This possibility has already been put forward by Agmon²⁸ in 1990, in connection with a dynamic Stokes shift in coumarin, asking the question ‘is it only relaxation?’. Examples of such a situation have been encountered with 4-cyanofluorazene²⁹ (FPP4CN) and 1-*tert*-butyl-6-cyano-1,2,3,4-tetrahydroquinoline³⁰⁻³² (NTC6). In these molecules, having a rigidified configuration such as that present with CVL, an activated ICT process takes place in *n*-hexane, in which orientational dielectric solvation does not play a role.

Recently, Li and Maroncelli reported photostationary fluorescence spectra and decays (time resolution 5 ps) of CVL in a series of aprotic solvents with different polarity (from *n*-hexane to

PC) at 25 °C.¹³ A solvatochromic analysis of the fluorescence spectra of CVL resulted in the dipole moments $\mu_e(\text{LE}) = 9\text{-}12$ D and $\mu_e(\text{ICT}) = 24$ D, similar to the values of Karpiuk (11 and 25 D)² mentioned above, although a different method was used.³³ It was pointed out that the 24 D for $\mu_e(\text{ICT})$ is equivalent to a distance of 5.0 Å between the centres of gravity of the positive and negative unit charges, comparable with the 5.6 Å between the centers of mass of the D and A units in CVL. The conclusion was then made that a full electron is transferred between the D (DMA) and A (6DMAPd) moieties of CVL during the LE \rightarrow ICT reaction in the series of solvents investigated.¹³

LE and ICT fluorescence decays of CVL were measured at 25 °C in a series of media with different polarities, from *n*-butyl acetate (BAC, $\epsilon^{25} = 4.95$) to PC ($\epsilon^{25} = 65$), as well as in methyl acetate (MAC, $\epsilon^{25} = 6.88$)/acetone ($\epsilon^{25} = 20.82$) and PC/MeCN mixtures.¹³ In the low-polarity solvents BAC to THF, the decays are single exponential, interpreted as showing that an ICT reaction does not take place, confirming the findings² of Karpiuk.⁶ In the more polar solvents dichloromethane (DCM, $\epsilon^{25} = 8.51$) to PC, the LE and ICT decays are double exponential with times τ_1 and τ_2 ($\tau_1 > \tau_2$, see below), in accordance with a two-state LE \rightleftharpoons ICT model, and an additional component attributed to impurity fluorescence. The time τ_2 decreases when the solvent polarity becomes larger, from 70 ps in DCM to 8 ps in MeCN. From these decays, the two times τ_1 and τ_2 and also their amplitude ratio were extracted, giving the forward (k_a) and backward (k_d) rate constant of the LE \rightleftharpoons ICT equilibrium and hence the change in free enthalpy $\Delta G = -RT\ln(k_a/k_d)$.^{13,34} ΔG ranges between 14 kJ/mol (extrapolated) for *n*-hexane to -10 kJ/mol for PC. With CVL in MeCN, for example, $\Delta G = -9.8$ kJ/mol. This value is larger than the -3.3 kJ/mol estimated in ref 24, but much smaller than the previous ΔG of -57 kJ/mol in ref 2.

The time-resolved fluorescence spectra of CVL in acetone and *n*-propyl cyanide (PrCN) exhibit an approximate isoemissive point. Although it was concluded in ref 13 that the ICT reaction of CVL in the various media is solvent-controlled, the appearance of such isoemissive points is not to be expected when solvent relaxation would be the determining factor, which then should lead to time-dependent spectral shifts (dynamic Stokes shifts).^{35,36} The same interpretation can also be found in reference 25 of ref 13, which states that a dynamic Stokes shift in a solvent with slow solvation responses prevents the appearance of an isoemissive point.¹³

In the PC/MeCN mixtures studied,¹³ the dielectric properties and thus also ΔG (-10 ± 1 kJ/mol) remain more or less constant. The decrease in the rate constant k_a of the LE \rightarrow ICT reaction from 78 to 45 $\times 10^9$ s⁻¹ when the PC/MeCN ratio becomes larger (4 mixtures, from 1:4 to 4:1) will therefore be caused by an increase of the activation barrier E_a . In these mixtures, $\langle \tau_{\text{sr}} \rangle$

becomes larger, from 0.37 to 1.25 ps, as does the viscosity: from 0.45 to 1.40 cP. The rate constant k_a is sensitive to the polarity as well as the viscosity (friction) of the solvent, which is interpreted as showing that an adiabatic electron transfer (ET) occurs. This ET process is primarily determined by solvent polarization modes, although it was also mentioned that viscosity and mean solvation time $\langle\tau_{sr}\rangle$ are proportional to each other.¹³ Nevertheless, the statement was made that in highly polar media, rates are correlated to solvation times in a manner that indicates that the reaction is a solvent-controlled electron transfer on an adiabatic potential surface having a modest barrier.¹³ The photophysical behavior of CVL in room temperature ionic liquids (ILs) has over the last years attracted considerable attention. Contradictory reports have appeared concerning the presence or absence of excitation wavelength dependence^{11,12,14,37-43} and a ‘red-edge effect’³⁹ of CVL fluorescence in ionic liquids, see Supporting Information.

In the present paper, absorption and fluorescence spectra of CVL in solvents of different polarity are presented. The spectra and the picosecond fluorescence decays (LE and ICT) in MeCN are investigated as a function of temperature.

Experimental Section

CVL (Aldrich) was crystallized twice from acetone.^{2,24} This sample^{2,24} was further purified by HPLC, by which treatment no additional impurities were detected. The solvents, MeCN (Merck, Uvasol), ethyl acetate (EAC, Merck, for analysis), THF (Merck, Uvasol), ethyl cyanide (EtCN, Merck, for analysis), PrCN (Merck, for analysis), and *n*-hexane (Merck, Uvasol) were chromatographed over Al₂O₃. The solutions, with an optical density between 0.4 and 0.6 for the maximum of the first band in the absorption spectrum, were deaerated by bubbling with nitrogen for 15 minutes. Absorption spectra were run on a Cary 500 spectrometer and the fluorescence spectra were measured with a quantum-corrected modified⁴⁴ Fluoromax 3 spectrofluorometer. The treatment of the fluorescence spectra and the determination of the quantum yields have been reported elsewhere.^{9,44-51} For the spectral separation of the overall fluorescence band of CVL into its LE and ICT components, the following method was employed. The ICT emission spectrum of MGL in DBE was taken as the starting point and was shifted to the red in order to match the low-energy side of the CVL fluorescence spectrum in MeCN. It thereby became clear that the ICT band of CVL obtained in this manner was broader than that of MGL. The width of the MGL ICT band was therefore increased, by convolution with a Gauss function. Subtraction of the total fluorescence spectrum by the widened MGL ICT

band then resulted in the LE emission spectrum of CVL. The final separation of the LE and ICT contributions to the total fluorescence was achieved by iterative smoothing. The picosecond fluorescence decays were obtained by using time-correlated single-photon counting (SPC). The decay times were determined with an equipment (excitation wavelength around 272 nm) consisting of a mode-locked titanium-sapphire laser (Coherent, MIRA 900F) pumped by an argon ion laser (Coherent, Innova 415). This laser apparatus and the analysis procedure of the fluorescence decays have been described previously.^{9,44-48,49} The instrument response function of the laser SPC system has a full width at half maximum of ~19 ps. The triplet yield $\Phi(\text{ISC})$ of the CVL in MeCN at room temperature (22 °C) was measured by laser flash photolysis, employing energy transfer.⁵² The excitation wavelength was 355 nm (third harmonic of a Nd:YAG laser, Continuum Surelight) with perylene as quencher and benzophenone as triplet yield reference ($\Phi(\text{ISC}) = 1.00$).^{52,53} A control experiment was carried out in which anthracene in the triplet state was the energy donor and CVL the acceptor.⁵⁴ For the determination of the decadic molar absorption coefficient, a benzophenone sample was used in MeCN as the reference with $\epsilon^{\text{max}}(525 \text{ nm}) = 6600 \text{ mol}^{-1} \text{ dm}^3 \text{ cm}^{-1}$.⁵⁵

Results and Discussion

Absorption and Fluorescence Spectra. The absorption spectrum of CVL at 25 °C in *n*-hexane, showing two weak bands at 29260 and around 33000 cm^{-1} together with a much stronger band at 37230 cm^{-1} (Figure 1a), is similar to that in MeCN (Figure 1b). The fluorescence spectrum of CVL in *n*-hexane consists of a single emission band from a LE state (Figure 1a), with a maximum at 25750 cm^{-1} . In MeCN at 25 °C (Figure 1b), the fluorescence spectrum can be separated into two bands, LE and ICT, with maxima at 22680 and 16440 cm^{-1} . These and other spectral data are collected in Table 1. ICT fluorescence is also detected in EAC and THF (Table 1),⁶ different from ref 2, see Figures S1 and S2 in the Supporting Information.

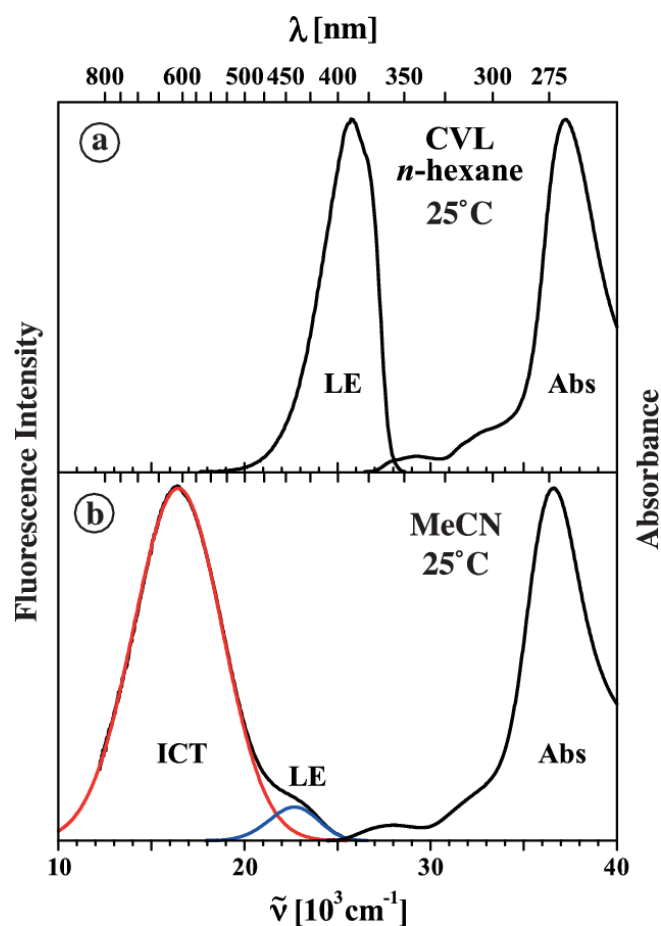


Figure 1. (a) Fluorescence (LE) and absorption (Abs) spectra of CVL in *n*-hexane at 25 °C. The fluorescence spectrum is attributed to the single emission from a locally excited (LE) state. (b) Fluorescence (LE + ICT) and absorption (Abs) spectra of CVL in acetonitrile (MeCN) at 25 °C. The fluorescence spectrum shows dual fluorescence from a LE and an intramolecular charge transfer (ICT) state, see text. Excitation wavelength: (a) 300 nm, (b) 330 nm.

Table 1. Data Obtained from the Fluorescence and Absorption Spectra of CVL in a Series of Solvents at Different Temperatures

Solvent ^a	<i>n</i> -hexane	EAC	THF	PrCN	EtCN	MeCN	MeCN	MeCN
T (°C)	25	25	25	25	25	25	-45	75
ϵ	1.88	5.99	7.39	24.2	29.2	36.7	50.2	30.3
$\tilde{\nu}^{\max}$ (Flu) (cm ⁻¹)	25750	23590	23820	17970	17390	16370	15870	16970
$\tilde{\nu}^{\max}$ (LE) (cm ⁻¹)	25750	23850	23990	23260	23070	22680	22100	22860
$\tilde{\nu}^{\max}$ (ICT) (cm ⁻¹)		20790	20760	18000	17400	16440	15840	16970
Φ (LE)						0.00038		
Φ' (ICT)						0.0070		
Φ' (ICT)/ Φ (LE)	0.0	0.61	0.41	6.7	10.9	18.3	12.4	8.8
Φ (ISC)						0.015 ^e		
Φ (IC) ^b						0.98		
$\tilde{\nu}^{\max}$ (S ₁ ,abs) (cm ⁻¹)	29260	28480	28450	28070	28060	28000	27810	28130
$\tilde{\nu}^{\max}$ (S ₃ ,abs) (cm ⁻¹)	37230	36860	36790	36630	36580	36590	36700	36550
OD(S ₃)/OD(S ₁) ^c	22.3	21.7	20.9	21.6	21.3	22.5	22.1	22.7
E (S ₁) (cm ⁻¹) ^d	28050	26610	26650	25870	25550	25500	25380	25880

^aSolvents: EAC (ethyl acetate), THF (tetrahydrofuran), PrCN (*n*-propyl cyanide), EtCN (ethyl cyanide), and MeCN (acetonitrile). ^b Φ (IC) = 1 - Φ (LE) - Φ' (ICT) - Φ (ISC). ^cRatio of the optical densities (OD) at the maxima of the S₃ and S₁ absorption bands, listed in the Table. ^dCrossing point of the fluorescence and absorption spectra (cf. Figure 1). ^eThe decadic molar absorption coefficient $\epsilon_T = 3750 \text{ mol}^{-1}\text{dm}^3\text{cm}^{-1}$ at the absorption maximum (470 nm) of the triplet-triplet absorption spectrum of CVL in MeCN.

Triplet-Triplet Absorption. Intersystem Crossing Yield Φ (ISC) of CVL in MeCN. The triplet yield Φ (ISC) of CVL in MeCN equals 0.015 ± 0.003 (Table 1). This value is small, but well reproducible. The yield Φ (IC) of internal conversion (IC) amounts to 0.98, as determined from Φ (IC) = 1 - Φ (LE) - Φ' (ICT) - Φ (ISC), see Table 1. This shows that IC is the main deactivation process for CVL in the S₁ state in MeCN. In the experiments with anthracene as the triplet energy donor, the CVL concentration at which all the anthracene was quenched cannot be reached and hence only an upper limit of 0.04 was estimated for Φ_{ISC} . For determination of the triplet-triplet absorption spectrum (Figure 2), the transient absorption signal was measured in the absence and presence of air. The difference signal was taken as the triplet transient, with a typical lifetime of 200-400 μs . In the 440-450 nm range an increase was detected on a 5 μs timescale, which must originate from the CVL triplet. In air-saturated samples, a long-lived transient species was observed, and this constituted 30-50 percent of the transient absorption signal measured in the deoxygenated sample. Even after several ten thousand 40 mJ laser flashes, the absorption spectrum of CVL in MeCN did not change appreciably, except in the case of the air-saturated sample, for which a weak blue coloration was found.

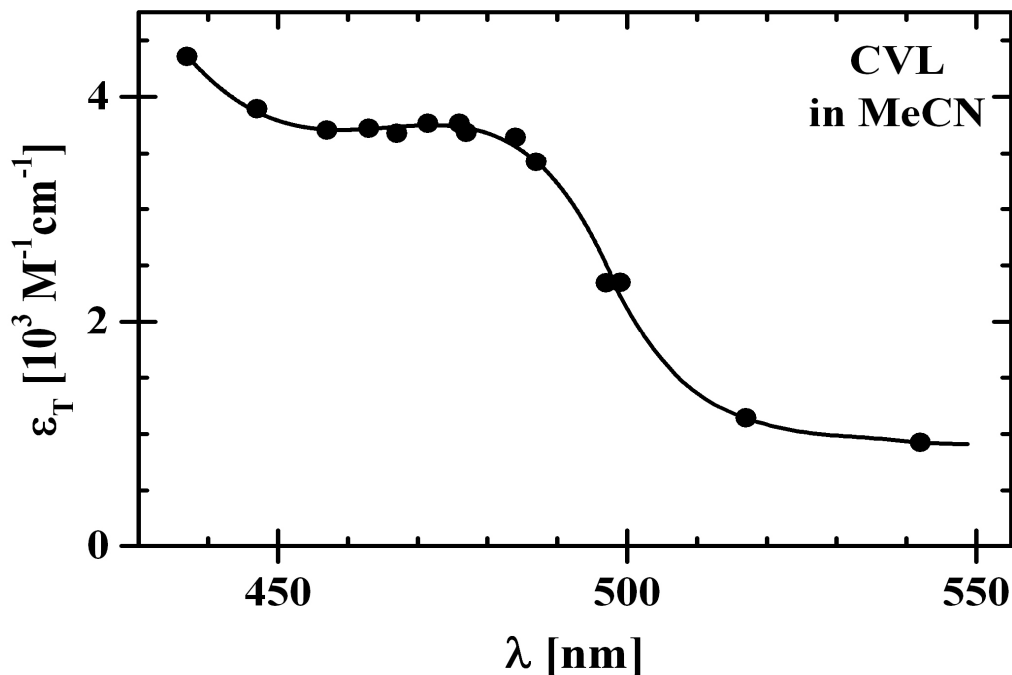


Figure 2. Triplet-triplet transient absorption spectrum of CVL in acetonitrile (MeCN) at room temperature (22 °C), see text. At the absorption maximum (470 nm), the decadic molar absorption coefficient $\varepsilon_T = 3750 \text{ mol}^{-1} \text{ dm}^3 \text{ cm}^{-1}$.

Solvatochromic Measurements. In order to determine the dipole moments of the LE and ICT states of CVL, the maxima $\tilde{\nu}^{\max}(\text{LE})$ and $\tilde{\nu}^{\max}(\text{ICT})$ of its fluorescence bands were measured in a series of solvents, from the nonpolar *n*-hexane ($\varepsilon^{25} = 1.88$) to the strongly polar MeCN ($\varepsilon^{25} = 36.7$), see Table 2.

Table 2: Fluorescence Maxima $\tilde{\nu}^{\max}$ of CVL, DMABN, and DIABN (in 1000 cm^{-1}) at 25 °C in a Series of Solvents

Solvent ^a	ε	n	$f(\varepsilon)$ $- f(n^2)$	$f(\varepsilon)$ $- \frac{1}{2}f(n^2)$	CVL		DMABN ^b $\tilde{\nu}^{\max}(\text{LE})$	DIABN ^c $\tilde{\nu}^{\max}(\text{ICT})$
					$\tilde{\nu}^{\max}(\text{LE})$	$\tilde{\nu}^{\max}(\text{ICT})$		
<i>n</i> -hexane (1)	1.88	1.372	0.000	0.092	25750	-	29430	
ethyl acetate (2)	5.99	1.370	0.200	0.292	23850	20780	27900	22260
tetrahydrofuran (3)	7.39	1.405	0.208	0.307	23990	20760	27800	22380
<i>n</i> -propyl cyanide (4)	24.2	1.382	0.281	0.375	23260	17990	27700	21090
ethyl cyanide (5)	29.2	1.363	0.293	0.384	23070	17400	27600	20870
acetonitrile (6)	36.7	1.342	0.306	0.393	22700	16440	27600	20490

^a Solvent acronyms: (2) EAC, (3) THF, (4) PrCN, (5) EtCN, (6) MeCN. ^b 4-(dimethylamino)benzonitrile. ^c 4-(diisopropylamino)benzonitrile.

From a plot of $\tilde{\nu}^{\max}(\text{LE})$ vs the solvent polarity parameter $g(\varepsilon, n) = f(\varepsilon) - f(n^2)$, $\mu_e(\text{LE})$ can be obtained, whereas $\mu_e(\text{ICT})$ can be determined by plotting $\tilde{\nu}^{\max}(\text{ICT})$ vs $g(\varepsilon, n) = f(\varepsilon) - \frac{1}{2}f(n^2)$ (eqs 1-3), see Figure 3a.^{30,49,51-54,56-60} This difference in $g(\varepsilon, n)$ appears while the ICT state is not populated by absorption in S_0 , but is formed from the directly excited LE precursor, as can be

seen from the time-resolved fluorescence spectra to be discussed below.^{30,49,51}

$$\tilde{\nu}^{\max}(\text{flu}) = -\frac{1}{2hc\rho^3} \mu_e(\mu_e - \mu_g) g(\varepsilon, n) + \text{const.} \quad (1)$$

$$f(\varepsilon) = \frac{\varepsilon - 1}{2\varepsilon + 1} \quad (2)$$

$$f(n^2) = \frac{n^2 - 1}{2n^2 + 1} \quad (3)$$

In eqs 1-3, μ_g and μ_e are the ground and excited state dipole moments, ε is the dielectric constant, n the refractive index, h is Planck's constant, c is the speed of light, and ρ the Onsager cavity radius of the solute.

Onsager Radius Employed for CVL. The method we generally have adopted in the determination of Onsager cavity radii ρ ,^{29,30,32,45,51,56,61-64} is to scale the crystal density data in such a manner that a value of 17 D results for $\mu_e(\text{ICT})$ of 4-(dimethylamino)benzonitrile (DMABN) from the solvatochromic and thermochromic analysis, giving an effective crystal density of 0.78, as described in detail in ref 49. The $\mu_e(\text{ICT}) = 17$ D for DMABN comes from time-resolved microwave induced conductivity (TRMC) experiments,⁸ which does not depend on the Onsager cavity radius and can hence be used as a calibration independent of solvatochromy.

The advantage of using such scaled crystal densities instead of, for example, an uniform density equal to 1.0, obviously is that the specific nature of the molecules is then better taken into account, provided that their crystal free volumes are comparable. From the density of 0.78, $\rho = 5.96 \text{ \AA}$ is calculated here for CVL. The crystal density of CVL $(1.19)^1$ is practically the same as that of DMABN (1.139) ,⁶⁵ supporting the validity of our approach.

Excited State Dipole Moments $\mu_e(\text{LE})$ and $\mu_e(\text{ICT})$ of CVL. In addition to the solvatochromic plots in Figure 3, the LE and ICT emission maxima of CVL are, as usual for us,^{29,30,32,45,49,51,56,61-64} also plotted against the $\tilde{\nu}^{\max}(\text{LE})$ of DMABN ($\mu_e(\text{LE}) = 10.6$ D) and the $\tilde{\nu}^{\max}(\text{ICT})$ of 4-(diisopropylamino)benzonitrile (DIABN) ($\mu_e(\text{ICT}) = 18$ D), respectively (Figure 3b).^{8,66} With this second procedure, the scatter in the data points is generally reduced by mutually compensating the specific solute/solvent interactions, as can clearly be seen in Figure 3.^{30,34,49,51,62} The calibration is based on TRMC dipole moments of DMABN, making the results much less dependent on the choice of ρ (eq 1).

From the slope of the plot of $\tilde{\nu}^{\max}(\text{LE, CVL})$ vs $f(\epsilon) - f(n^2)$, a dipole moment $\mu_e(\text{LE}) = 16.6$ D is calculated for CVL, whereas from the plot against $\tilde{\nu}^{\max}(\text{LE, DMABN})$ the nearly identical $\mu_e(\text{LE}) = 17.4$ D is obtained (Figure 3a). Similarly, $\mu_e(\text{ICT}) = 32.7$ D results from plotting $\tilde{\nu}^{\max}(\text{ICT, CVL})$ vs $f(\epsilon) - \frac{1}{2}f(n^2)$ and a comparable $\mu_e(\text{ICT}) = 34.3$ D is found from the plot against $\tilde{\nu}^{\max}(\text{ICT, DIABN})$, see Figure 3b and Table 3. Note that the LE dipole moment $\mu_e(\text{LE})$ is very large and that we know that it is nevertheless not an ICT state, within the context of our definition of LE and ICT.⁷⁻⁹ For DMABN, $\mu_e(\text{LE})$ is also already relatively large (10.6 D),⁸ which likewise does not mean that it is the dipole moment of an ICT state.^{8,44}

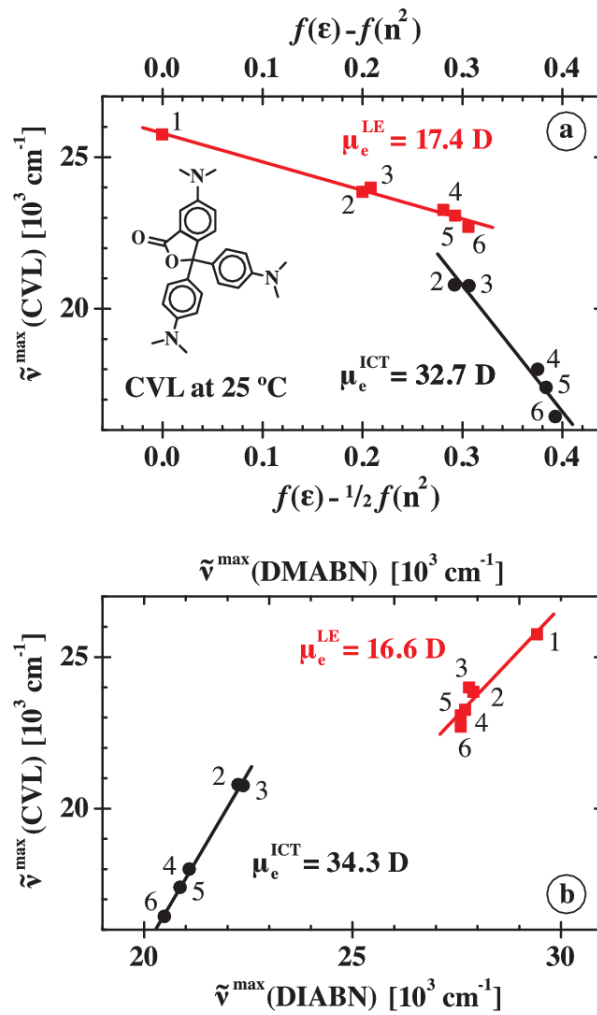


Figure 3. Solvatochromic plots of the LE and ICT fluorescence maxima $\tilde{\nu}^{\max}(\text{LE})$ and $\tilde{\nu}^{\max}(\text{ICT})$ of CVL vs (a) the solvent polarity parameters $g(\epsilon, n^2)$ and (b) $\tilde{\nu}^{\max}(\text{LE})$ of DMABN and $\tilde{\nu}^{\max}(\text{ICT})$ of DIABN (eqs 1-3). For LE, $g(\epsilon, n) = f(\epsilon) - f(n^2)$, whereas for ICT $g(\epsilon, n) = f(\epsilon) - \frac{1}{2}f(n^2)$, see Table 3 and text. The $\tilde{\nu}^{\max}$ data and the numbering of the solvents are given in Table 2. From the slopes of the plots, the LE and ICT dipole moments $\mu_e(\text{LE})$ and $\mu_e(\text{ICT})$, indicated in the Figures, are calculated (Table 3).

Table 3: Data from the Solvatochromic Analysis of the Fluorescence Maxima $\tilde{\nu}^{\max}$ (LE) and $\tilde{\nu}^{\max}$ (ICT) of CVL

	ρ (Å) ^a	μ_g (D) ^b	Slope (cm ⁻¹)	$\tilde{\nu}^{\max}$ (CVL) vs	μ_e (D) ^c
LE	5.96	6.0	-9410 ± 590 ^d	$f(\epsilon)-f(n^2)$	17.4 ± 0.4
LE	5.96	6.0	1.45 ± 0.24 ^e	$\tilde{\nu}^{\max}$ (LE,DMABN)	16.6 ± 1.1
ICT	5.96	6.0	-41700 ± 4400 ^f	$f(\epsilon)-\frac{1}{2}f(n^2)$	32.7 ± 1.6
ICT	5.96	6.0	2.33 ± 0.08 ^g	$\tilde{\nu}^{\max}$ (ICT,DIABN)	34.3 ± 0.6

^aOnsager radius (eq 1), determined from a density equal to 0.78, based on DMABN (ref 49). ^bGround state dipole moment, calculated by AM1; result scaled by μ_g (DMABN) = 6.6 D (ref 8). ^cICT or LE dipole moment (eq 1).

^dFrom a plot of $\tilde{\nu}^{\max}$ (LE) vs $f(\epsilon)-f(n^2)$, eqs 1-3, see Figure 3a. ^eFrom a plot of $\tilde{\nu}^{\max}$ (LE) vs $\tilde{\nu}^{\max}$ (LE) of DMABN (Figure 3b), with $\rho = 4.20$ Å, $\mu_g = 6.6$ D, from refs 49, 51, and 61. ^fFrom a plot of $\tilde{\nu}^{\max}$ (ICT) vs $f(\epsilon)-\frac{1}{2}f(n^2)$, eqs 1-3, see Figure 3a. ^gFrom a plot of $\tilde{\nu}^{\max}$ (ICT) vs $\tilde{\nu}^{\max}$ (ICT) of DIABN (Figure 3b), with $\rho = 4.68$ Å, $\mu_g = 6.8$ D and μ_e (ICT) = 18 D for DIABN, from refs 49 and 66.

Comparison of μ_e (LE) and μ_e (ICT) of CVL with Literature Data. In the solvatochromic analysis of ref 2, the LE and ICT fluorescence maxima $\tilde{\nu}^{\max}$ (LE) and $\tilde{\nu}^{\max}$ (ICT) of CVL are both plotted versus the solvent polarity parameter $f(\epsilon) - \frac{1}{2}f(n^2)$, see eqs 1-3, in contrast with our procedure described above. In this analysis, different Onsager radii were employed for the LE and ICT states of CVL: ρ (LE) = 3.6 Å and ρ (ICT) = 5.8 Å. This assumption was based on the notion the charges in the LE state are located (and displaced) only within the 6DMAPd moiety, whereas for the ICT state the charges are delocalized over 6DMAPd and the DMAs in the CVL molecule. It was then considered to be reasonable that the solvation of the LE state involves primarily the solvent molecules surrounding 6DMAPd. Here, an Onsager radius $\rho = 5.96$ Å is taken for the LE as well as the ICT state (Table 3), adopting the point of view that the same cavity has to be created in the solvent for both states, due to their identical molecular volume. Note that our $\rho = 5.96$ Å is similar to the ρ (ICT) = 5.8 Å of ref 2.

In ref 2, μ_e (LE) = 10.7 D and μ_e (ICT) = 25.2 D are reported for CVL. The dipole moment $\mu_g = 5.5$ D (AM1)² is somewhat smaller than that used here ($\mu_g = 6.0$ D, Table 3). The slopes of the plots of $\tilde{\nu}^{\max}$ (LE) and $\tilde{\nu}^{\max}$ (ICT) vs $g(\epsilon, n) = f(\epsilon) - \frac{1}{2}f(n^2)$ are -10645 cm⁻¹ (LE) and -32910 cm⁻¹ (ICT), respectively. The LE slope is somewhat larger than our result of -9410 cm⁻¹, whereas the ICT slope is considerably smaller than our 41700 cm⁻¹ (Table 3). Maroncelli obtained similar dipole moments μ_e (LE) = 9-12 D and μ_e (ICT) = 24 D, also taking $\rho = 3.6$ Å for LE and $\rho = 5.8$ Å for ICT, from Karpiuk,² with $\mu_g = 6.0$ D (B3LYP/6-311G(d)).¹³ The solvatochromic method employed in ref 13 is different from that used here and in ref 2 and is therefore not directly comparable.

As described above, the dipole moments calculated from our solvatochromic analysis of CVL are clearly larger: $\mu_e(\text{LE}) = 17 \text{ D}$ and $\mu_e(\text{ICT}) = 33 \pm 1 \text{ D}$ (Table 3). On inspection of the $\tilde{\nu}^{\text{max}}$ data of refs 2 and 13 (Table S1), it is seen that our $\tilde{\nu}^{\text{max}}(\text{LE})$ and $\tilde{\nu}^{\text{max}}(\text{ICT})$ (Table 2) are shifted more to the red than the previous ones.^{2,13} As this red-shift grows when the solvent polarity becomes higher, the slopes of our plots are larger, leading to an increase of the dipole moments, especially $\mu_e(\text{ICT})$. There is no difference in the absorption maxima $\tilde{\nu}^{\text{max}}(\text{abs})$, see Table S1. These red-shifts are most probably due to problems with the spectral calibration of the fluorimeters employed in the experiments, as well as with the subtraction procedure used to separate the fluorescence spectra into its LE and ICT components. The impact of the differences in this calibration is much more severe for the ICT than for the LE fluorescence maxima, as the $\tilde{\nu}^{\text{max}}(\text{ICT})$ are in the red part of the spectrum, such as $\tilde{\nu}^{\text{max}}(\text{ICT}) = 16440 \text{ cm}^{-1}$ in MeCN at 25 °C (Table 2). We have circumvented these problems, and also to an important extent that of $\rho(\text{Onsager})$, by plotting the $\tilde{\nu}^{\text{max}}$ of CVL vs those of DIABN and basing ourselves on the $\mu_e(\text{ICT})$ of DMABN determined by TRMC,⁸ a method independent of solvatochromy, as mentioned above. We therefore think, that our values for the $\mu_e(\text{LE})$ and $\mu_e(\text{ICT})$ of CVL more correspond to reality. Over the years, in line with the present spectral calibration problems, it has been our experience, that fluorescence spectra in the literature are rarely, if at all, identical.

Temperature Dependence of CVL Fluorescence in MeCN. The fluorescence and absorption spectra of CVL in MeCN have been studied as a function of temperature. Those at the two extreme temperatures, -45 and 75 °C, are shown in Figure 4. The ICT fluorescence maxima $\tilde{\nu}^{\text{max}}(\text{ICT})$ increase from 15840 to 16970 cm^{-1} over this temperature range, a blue-shift of 1120 cm^{-1} (Table 2). The corresponding shift of $\tilde{\nu}^{\text{max}}(\text{LE})$, from 22100 to 22860 cm^{-1} , is with 760 cm^{-1} considerably smaller, as to be expected because of the much smaller dipole moment $\mu_e(\text{LE})$ of 17 D as compared with the $\mu_e(\text{ICT})$ of 33 D (Table 3), see eq 1. Both blue shifts are caused by the decrease in solvent polarity of MeCN upon heating: the dielectric constant ϵ goes down from 50.2 at -45 °C to 30.3 at 75 °C (Table 1) and the refractive index n decreases from 1.378 to 1.317 between these temperatures.

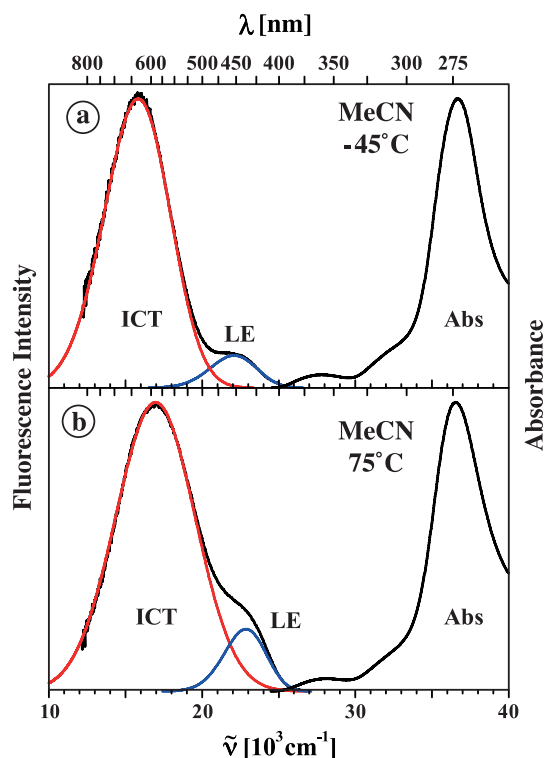
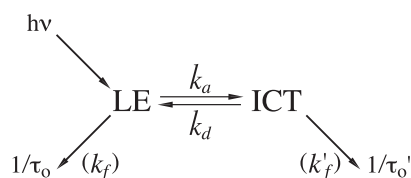


Figure 4. Fluorescence (LE + ICT) and absorption (Abs) spectra of CVL in acetonitrile (MeCN) at (a) -45 °C. and (b) at 75 °C. The fluorescence spectra show dual fluorescence from a locally excited (LE) and an intramolecular charge transfer (ICT) state, see text. Excitation wavelength: 330 nm.

$\Phi'(\text{ICT})/\Phi(\text{LE})$ as a Function of Temperature. Stevens-Ban Plot. For systems with two kinetically interconverting states, such as LE and ICT in Scheme 1, the fluorescence quantum yield ratio $\Phi'(\text{ICT})/\Phi(\text{LE})$ can be expressed by the following equations (eqs 4-6).^{30,31,49,56,67}

$$\Phi'(\text{ICT})/\Phi(\text{LE}) = k'_f(\text{ICT})/k_f(\text{LE}) \{k_a/(k_d + 1/\tau'_o(\text{ICT}))\} \quad (4)$$



Scheme 1

In Scheme 1 and eqs 4-6, k_a and k_d are the rate constants of the forward and backward ICT reaction, $\tau_0(\text{LE})$ is the fluorescence lifetime of the model compound (no ICT), $\tau'_0(\text{ICT})$ is the fluorescence lifetime of the ICT state (no back ICT). $k_f(\text{LE})$ and $k'_f(\text{ICT})$ are the radiative rate constants. The reciprocal lifetimes are equal to the sums of their radiative and nonradiative rate constants.

Temperature Limits. When $k_d \gg 1/\tau'_0(\text{ICT})$, the high-temperature limit (HTL), with a small ICT reaction enthalpy difference $-\Delta H$,⁵⁶ eq 4 simplifies to eq 5.

$$\Phi'(\text{ICT})/\Phi(\text{LE}) = k'_f(\text{ICT})/k_f(\text{LE}) k_a/k_d \quad (5)$$

Alternatively, when $k_d \ll 1/\tau'_0(\text{ICT})$, the low-temperature limit (LTL) (large $-\Delta H$),⁶⁷ eq 6 holds.

$$\Phi'(\text{ICT})/\Phi(\text{LE}) = (k'_f(\text{ICT})/k_f(\text{LE})) k_a \tau_o(\text{ICT}) \quad (6)$$

At 25 °C, $\Phi'(\text{ICT})/\Phi(\text{LE}) = 18.3$ (Table 1). This value is closer to the result of ref 13 (13.3) than that of ref 2 (6.5).⁶⁸ The data for $\Phi'(\text{ICT})/\Phi(\text{LE})$ of CVL in MeCN between -45 and 75 °C are plotted in Figure 5 as a Stevens-Ban (SB) plot, $\ln(\Phi'(\text{ICT})/\Phi(\text{LE}))$ vs $1000/T$. The activation energy $E_a(\text{SB}) = 8.7$ kJ/mol of k_a (LTL-slope, eq 6) and the enthalpy difference $\Delta H(\text{SB}) = -23.9$ kJ/mol (HTL-slope, eq 5) are determined by a nonlinear fitting (eq 4) of $\ln(\Phi'(\text{ICT})/\Phi(\text{LE}))$ over the whole temperature range, with the reasonable approximation that $(k'_f(\text{ICT})/k_f(\text{LE}))$ is temperature independent, as both rate constants will depend on the solvent refractive index. The activation energy of k_d , $E_d(\text{SB}) = E_a(\text{SB}) - \Delta H(\text{SB}) = 32.6$ kJ/mol. One can thus safely conclude that the ICT reaction of CVL in MeCN is not barrierless. An inspection of Figure 5 shows that the maximum of $\ln(\Phi'(\text{ICT})/\Phi(\text{LE}))$ occurs at around 10 °C. At this maximum, $k_d = 1/\tau_o(\text{ICT})$,^{49,56,65,69} which means that at 25 °C the HTL condition $k_d \gg 1/\tau_o(\text{ICT})$ and eq 5 are just barely fulfilled. A comparison of the data of CVL with corresponding photostationary data for DMABN in MeCN is of interest: $\Delta H(\text{SB}) = -23.2$ kJ/mol, $E_a(\text{SB}) = 7.7$ kJ/mol, $E_d(\text{SB}) = 30.9$ kJ/mol, similar to those of CVL.⁴⁴ Data for E_a , E_d , or ΔH for CVL in MeCN have previously not been reported in the literature. Only results for ΔG are available.^{2,13} These data will be compared in a later section with those derived from the analysis of fluorescence decays as a function of temperature (Table 4).

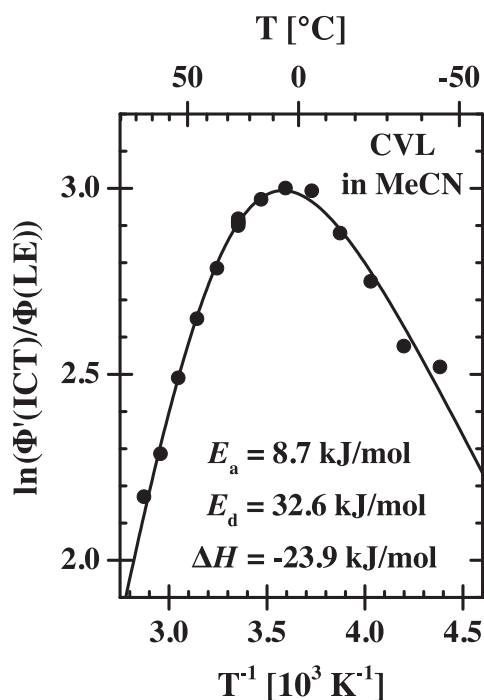


Figure 5. Stevens-Ban (SB) plot of $\Phi'(\text{ICT})/\Phi(\text{LE})$ vs $1000/T$ of CVL in MeCN, see eq 1. The activation energies $E_a(\text{SB})$ and $E_d(\text{SB})$ of the forward and backward reactions in the $\text{LE} \rightleftharpoons \text{ICT}$ equilibrium (Scheme 1) and the enthalpy difference $\Delta H(\text{SB}) = E_a(\text{SB}) - E_d(\text{SB})$ are indicated in the Figure. The thermodynamic data obtained here from the photostationary experiments are characterized in this caption and in the text with (SB), to differentiate them from the corresponding data derived from fluorescence decays in a later section.

Double Exponential LE and ICT Fluorescence Decays of CVL in MeCN at 25 °C. Global

Analysis. The LE and ICT picosecond fluorescence decays of CVL in MeCN at 25 °C are depicted in Figure 6. From a global analysis^{44,71,72} of these decays, two times are determined: $\tau_2 = 9.2$ ps and $\tau_1 = 1180$ ps (eqs 7-9) with $A_{12}/A_{11} = 35.3$. The ICT fluorescence response function shows a growing in (Figure 6), with an amplitude ratio A_{22}/A_{21} equal to -1.00 (eq 8). When $A_{21} = -A_{22}$, then the concentration $[ICT] = 0$ at $t = 0$ (eq 8). This means that the ICT state does not yet exist at the moment of light absorption in S_0 : LE is the precursor of ICT.⁴⁴ Comparable decay times have been observed previously for CVL in MeCN at 25 °C: $\tau_2 = 8$ ps, $\tau_1 = 1200$ ps with $A_{12}/A_{11} = 49.4$ in ref 13 and τ_2 is 7.8 ps (LE) and 9.5 ps (ICT) in ref 24. The LE decays appearing in the literature are not double exponential. An additional time of 0.5 ps is found in ref 24 and the decays in ref 13 are triple exponential, with a small amplitude middle time of around 200 ps, attributed to impurities.

$$i_f(LE) = A_{11}\exp(-t/\tau_1) + A_{12}\exp(-t/\tau_2) \quad (7)$$

$$i_f(ICT) = A_{21}\exp(-t/\tau_1) + A_{22}\exp(-t/\tau_2) \quad \text{with } A_{21} = -A_{22} \quad (8)$$

$$A = A_{12}/A_{11} \quad (9)$$

As $\tau_2 \ll \tau_1$, the amplitude ratio $A = A_{12}/A_{11}$ (eq 9) of the LE decay (Figure 6) is practically equal to the ratio of the forward and backward ICT rate constants k_a/k_d (Scheme 1, eq 7).⁴⁴ In such a case, also $1/\tau_2 = k_a + k_d$.^{44,70} From $\tau_2 = 9.2$ ps and $A_{12}/A_{11} = 35.3$, $k_a = 106 \times 10^9 \text{ s}^{-1}$ and $k_d = 3.0 \times 10^9 \text{ s}^{-1}$ are then calculated. These approximate but in this case accurate⁷³ results already show that not only the LE \rightarrow ICT forward reaction of CVL in MeCN at 25 °C is very fast, but that this is also still the case for the ICT \rightarrow LE back reaction, a clear indication that ΔH is not extremely large. For comparison, $k_d = 0.47 \times 10^9 \text{ s}^{-1}$ and $\Delta H = -27.0$ kJ/mol for DMABN in MeCN at 25 °C.⁴⁴ See Figure 9 and Table 6, below, with $\Delta H = -19.6$ kJ/mol for CVL in MeCN.

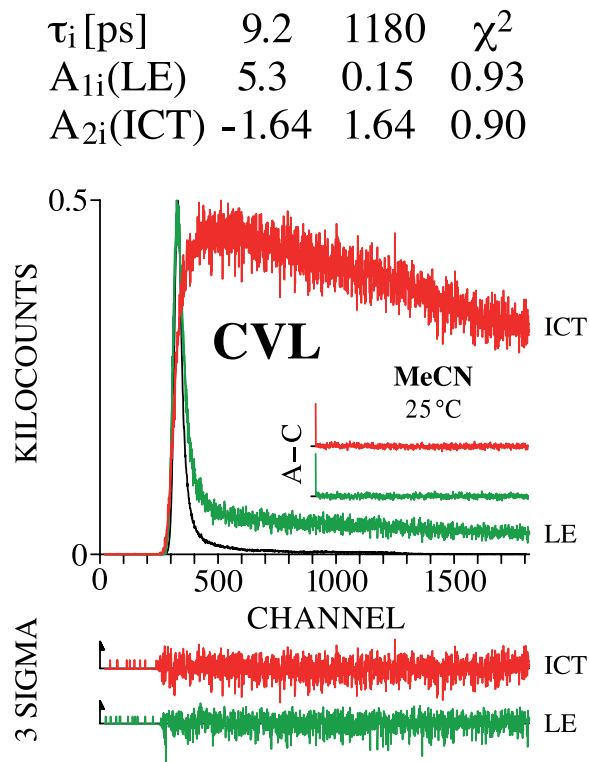


Figure 6. Picosecond fluorescence decays of CVL in MeCN at 25 °C. The decays are measured at 440 nm and 650 nm, with a time resolution of 0.4969 ps/channel and a time window of 1500 effective channels. The 440 nm decay is attributed to LE, that at 650 nm to ICT, see Figure 1b. The LE and ICT decays are analyzed simultaneously (global analysis), resulting in decay times $\tau_2 = 9.2$ ps and $\tau_1 = 1180$ ps, with amplitudes $A_{1i}(\text{LE})$ and $A_{2i}(\text{ICT})$, see eqs 7-9. The shortest time τ_2 is listed first. Excitation wavelength: 272 nm. The weighted deviations sigma, the autocorrelation functions A-C, and the values for χ^2 are also indicated.

Fluorescence Decays in MeCN as a Function of Temperature: -45 to 75 °C. The LE and ICT fluorescence decays of CVL in MeCN at -45 °C (Figure 7a) and 75 °C (Figure 7b) are also double exponential, which is the case over the entire temperature range (Table 5). The ICT amplitude ratio A_{22}/A_{21} is with -0.99 (-45 °C) and -0.97 (75 °C) close to the value -1.00 observed at 25 °C, from which it can again safely be deduced that at all temperatures investigated the ICT state is not directly prepared by absorption in S_0 , but is formed from LE as the precursor, similar to the situation at 25 °C discussed in the previous section (Figure 6).

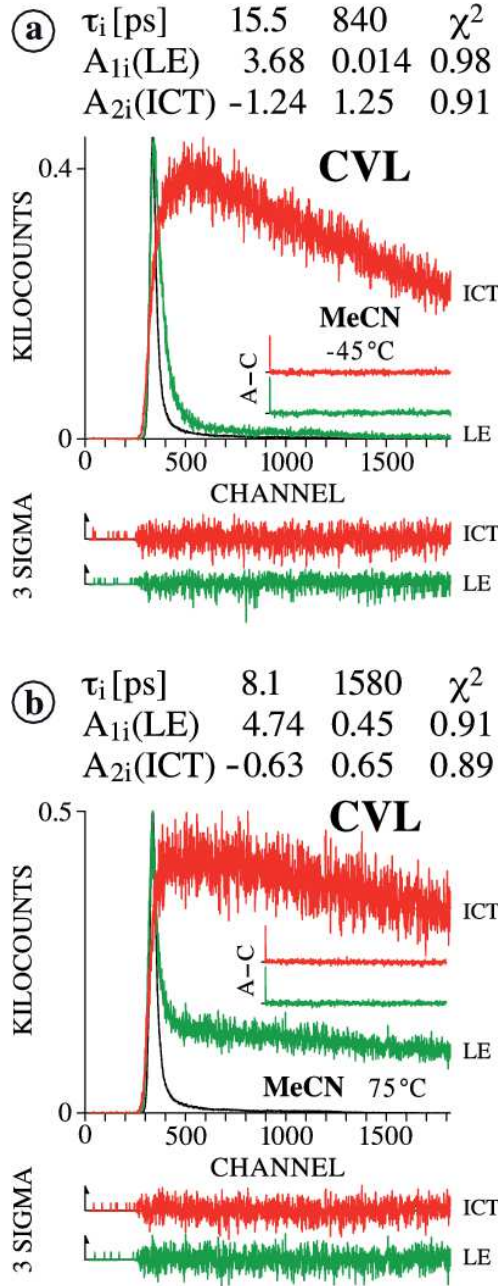


Figure 7. Picosecond fluorescence decays of CVL in MeCN at (a) -45 °C and (b) 75 °C. The decays are measured at 440 nm and 650 nm, with a time resolution of 0.4969 ps/channel and a time window of 1500 effective channels. The 440 nm decay are attributed to LE, those at 650 nm to ICT, see Figure 1b. The LE and ICT decays are analyzed simultaneously (global analysis), resulting in decay times τ_2 and τ_1 , with amplitudes $A_{1i}(\text{LE})$ and $A_{2i}(\text{ICT})$, see eqs 7-9. The shortest time τ_2 is listed first. Excitation wavelength: 272 nm. See the caption of Figure 6.

Decay Times τ_2 and τ_1 and Amplitude Ratios A_{12}/A_{11} as a Function of Temperature. The decay time τ_2 of CVL in MeCN decreases from 15.5 ps at -45 °C to 8.1 ps at 75 °C, whereas τ_1 increases from 0.84 to 1.58 ns over this temperature range (Figure 8). The amplitude ratio A_{12}/A_{11} continually becomes smaller from 263 to 10.5, when going from -45 to 75 °C, see Table 4.

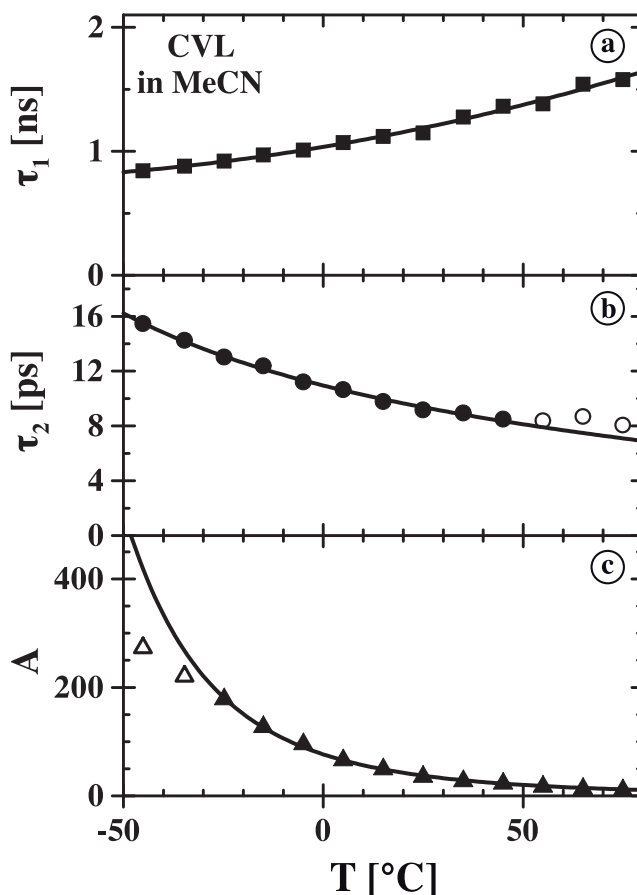


Figure 8. CVL in MeCN. Plots as a function of temperature of the fluorescence decay times τ_1 (a, ■) and τ_2 (b, ○ and ●), see eqs 7 and 8, and (c, Δ and ▲) the LE amplitude ratio A_{12}/A_{11} (eq 9).

LE Lifetime $\tau_0(\text{LE}) = 39$ ns for CVL in MeCN. To determine the ICT reaction parameters k_a , k_d , $\tau_0(\text{LE})$, and $\tau_o(\text{ICT})$ (Scheme 1) from the decay times τ_2 and τ_1 together with the LE amplitude ratio A_{12}/A_{11} (eq 8), a fourth input is necessary. As usual,^{8,25,29,30,31,35,44-46,48,51,56,61-64,66,67,70,72} this is the fluorescence lifetime $\tau_0(\text{LE})$, which is equal to the LE fluorescence lifetime under the condition that an ICT reaction does not take place ($k_a = 0$). For CVL this is the case in solvents less polar than EAC, such as *n*-hexane (Figure 1a, Tables 1 and 2).

The LE emission spectrum of CVL in low-polarity solvents such as *n*-hexane and diethyl ether (DEE) is identical to that of 6DMAPd.^{2,13,24} Also the LE fluorescence lifetimes $\tau_0(\text{LE})$ of CVL and 6DMAPd in the solvent series between *n*-hexane and THF have comparable values, such as 15.5 ns (CVL)² and 24.7 ns (6DMAPd)¹⁶ in DEE. We therefore adopt the $\tau_0(\text{LE}) = 39.2$ ns of 6DMAPd in MeCN¹⁶ as the lifetime $\tau_0(\text{LE}) = 39$ ns of the LE state of CVL in MeCN.⁷⁴ Even for EAC and THF, in which solvents we have observed dual (LE + ICT) fluorescence of CVL (Figures S1 and S2), similar fluorescence decay times τ_1 are found: 19.3 or 15 ns (CVL)^{2,13} and 27.9 ns (6DMAPd)¹⁶ in EAC, 22.4 ns (CVL)² and 25.1 ns (6DMAPd)¹⁶ in THF. Note that a surprisingly much smaller τ_1 of 4.5 ns has been reported for CVL in THF.¹³

ICT Reaction Rate Constants k_a and k_d , Lifetime $\tau_o(\text{ICT})$. The ICT rate constants k_a and k_d , as well as the lifetime $\tau_o(\text{ICT})$ of CVL in MeCN, calculated from τ_1 , τ_2 , and A_{12}/A_{11} (eqs 7-9) with $\tau_0(\text{LE}) = 39$ ns, are listed in Table 4. At 25 °C (Figure 6), $k_a = 106 \times 10^9 \text{ s}^{-1}$, $k_d = 3.0 \times 10^9 \text{ s}^{-1}$ and $\tau_o(\text{ICT}) = 1.15$ ns (Table 4). Upon heating from -45 to 75 °C, the forward rate constant k_a becomes larger, from 64×10^9 to $114 \times 10^9 \text{ s}^{-1}$, whereas the backward rate constant k_d as usual increases more strongly, from 0.23×10^9 to $10.6 \times 10^9 \text{ s}^{-1}$ between these temperatures. Also the lifetime $\tau_o(\text{ICT})$ becomes larger when going from -45 to 75 °C,⁷⁵ which will be further discussed below. A similar temperature dependence of $\tau_o(\text{ICT})$ has been observed with DMABN in MeCN.⁴⁴

Table 4. Decay Parameters of CVL in Acetonitrile (MeCN) as a Function of Temperature

T (°C)	τ_2 (ps)	τ_1 (ns)	A_{12}/A_{11}	k_a (10^9 s^{-1}) ^{a,b}	k_d (10^9 s^{-1}) ^{a,c}	$\tau_o(\text{ICT})$ (ns) ^a	ΔG (kJ/mol) ^d	ΔG_a^\ddagger (kJ/mol) ^e
74.9	8.1 (7.1)	1.58 (1.60)	10.7 (12.0)	114 (130)	10.55 (10.75)	1.45 (1.48)	-6.9 (-7.2)	12.0 (11.6)
65.0	8.7 (7.5)	1.54 (1.50)	12.9 (14.6)	107 (125)	8.21 (8.45)	1.43 (1.41)	-7.2 (-7.6)	11.8 (11.3)
54.9	8.4 (7.9)	1.38 (1.42)	17.0 (18.1)	113 (120)	6.55 (6.55)	1.31 (1.34)	-7.8 (-7.9)	11.2 (11.0)
45.0	8.5	1.36	22.7	113	4.91	1.31	-8.3	10.8
35.1	8.9	1.28	27.1	108	3.93	1.23	-8.5	10.5
25.0 ^f	9.2	1.18	35.3	106	2.95	1.15	-8.9	10.1 ^g
15.0	9.8	1.12	49.3	100	2.00	1.10	-9.4	9.8
5.0	10.6	1.07	65.8	92.6	1.38	1.05	-9.7	9.6
-5.0	11.2	1.01	95.5	88.3	0.90	1.00	-10.2	9.2
-15.0	12.4	0.97	127	80.1	0.62	0.96	-10.5	9.0
-24.8	13.0	0.92	178	76.4	0.42	0.92	-10.8	8.7
-34.7	14.3 (14.2)	0.88 (0.88)	221 (267)	69.8 (70.3)	0.31 (0.26)	0.88 (0.88)	-10.8 (-11.1)	8.5 (8.4)
-45.1	15.5 (15.5)	0.84 (0.85)	273 (419)	64.4 (64.3)	0.23 (0.15)	0.84 (0.84)	-10.7 (-11.5)	8.2 (8.2)

^aIn the calculation of k_a , k_d , and $\tau_o(\text{ICT})$ from τ_2 , τ_1 , and A_{12}/A_{11} , the value $\tau_0(\text{LE}) = 39$ ns is adopted, see text.

^bThe value in parentheses is calculated from $E_a = 3.9$ kJ/mol and $k_a^0 = 4.95 \times 10^{11} \text{ s}^{-1}$ (Table 6). ^cThe value in parentheses is calculated from $E_d = 23.6$ kJ/mol and $k_d^0 = 3.68 \times 10^{13} \text{ s}^{-1}$ (Table 6). ^d $\Delta G = -RT \ln(k_a/k_d)$. ^e ΔG_a^\ddagger is calculated from k_a , employing the expression $k_a = kT/h e^{-\Delta G_a^\ddagger/RT}$, assuming that such an approach based on the vibration of a diatomic molecule ($h\nu = kT$) is valid here for a compound as large as CVL, in MeCN. ^fRef 2: $\tau_1 = 1.5$ ns, $\tau_2 = 7.8$ ps (LE) or 9.5 ps (ICT), with additional shorter decay times 0.5 ps or <0.3 ps (ref 2). Ref 13: $\tau_2 = 8$ ps, $\tau_1 = 1.2$ ns, $A_{12}/A_{11} = 49.4$, $\Delta G = -9.8$ kJ/mol. From these data for τ_2 , τ_1 , A_{12}/A_{11} , and $\tau_0(\text{LE}) = 39$ ns: $k_a = 1.23 \times 10^{11} \text{ s}^{-1}$, $k_d = 2.45 \times 10^9 \text{ s}^{-1}$, $\tau_o(\text{ICT}) = 1.18$ ns, and $\Delta G = -9.7$ kJ/mol. ^gRef 13: $\Delta G_a^\ddagger = 10.8$ kJ/mol; Ref 38: $\Delta G_a^\ddagger = 85.8$ kJ/mol from MD simulation.

Temperature Dependence of $\tau_o(\text{ICT})$ in MeCN. The observation that the lifetime $\tau_o(\text{ICT})$ of CVL in MeCN increases when going from -45 to 75 °C (Table 4) is at first sight surprising. The reciprocal of the ICT lifetime, $1/\tau_o(\text{ICT})$, is equal to the sum of three rate constants, $k'_f(\text{ICT})$ for fluorescence, $k'(\text{IC})$ for internal conversion (IC), and $k'(\text{ISC})$ for ISC (eq 10). It is hence clear that the temperature dependence of $\tau_o(\text{ICT})$ can in principle be an inherently complex issue. The last two processes IC and ISC are often activated in similar D/A systems,⁷⁶ which means that $k'(\text{ISC})$ and $k'(\text{IC})$ become larger upon heating (Arrhenius behavior), which would contribute to a shortening of $\tau_o(\text{ICT})$. Because $k'_f(\text{ICT})$ depends on the refractive index n , as n^p

with values for p between 2 and 3,^{44,76-78} it becomes smaller upon cooling, as n decreases when the temperature rises, for MeCN from 1.3780 at -45 °C to 1.3169 at 75 °C.^{79,80} Therefore, only when $k'_f(\text{ICT})$ is the dominant decay process, such as when $\Phi'(\text{ICT})$ is close to 1.0, $\tau_o(\text{ICT})$ would become longer at higher temperatures. For CVL in MeCN, however, $\Phi'(\text{ICT})$ is very small, 0.007 at 25 °C (Table 1). This means that the condition $k'_f(\text{ICT}) \sim n^p$ cannot be responsible for the drastic (72 percent) increase of $\tau_o(\text{ICT})$ between -45 and 75 °C.

$$1/\tau_o(\text{ICT}) = k'_f(\text{ICT}) + k'(\text{IC}) + k'(\text{ISC}) \quad (10)$$

Energy Gap Law and Temperature. A plausible explanation of the observed temperature dependence of $\tau_o(\text{ICT})$ of CVL in MeCN is the following. Over the range from 75 to -45 °C, the energy of the fluorescence maximum $\tilde{\nu}^{\text{max}}(\text{ICT})$ shifts from 16970 to 15840 cm⁻¹ (Table 1). This red-shift is caused, as mentioned above, by the increase in solvent polarity (from $\epsilon^{75} = 30.3$ to $\epsilon^{45} = 50.2$)⁸¹ and the large difference in the dipole moments $\mu_e(\text{ICT}) - \mu_g$ of ~28 D (eq 1 and Table 3). As a consequence, the energy gap (equal to $\tilde{\nu}^{\text{max}}(\text{ICT})$) between the ICT state and its corresponding Franck-Condon (FC) ground state $S_0(\text{FC})$ becomes smaller when the temperature is lowered, leading to a more efficient IC process (energy gap law)⁸²⁻⁸⁵ and hence to a shortening of $\tau_o(\text{ICT})$. There will not be an appreciable influence of the ICT- $S_0(\text{FC})$ energy gap on the ISC process, because this reaction proceeds isoenergetically between the ICT state and the CVL triplet manifold. Also $k'_f(\text{ICT})$ is not expected to be governed by the energy gap law: it depends on the solvent refractive index as n^p , with values for p between 2 and 3, as mentioned above. When ISC would be the predominant process, as previously reported for CVL in MeCN with $\Phi(\text{ISC}) \sim 1.0^5$ instead of our result of 0.015 (Table 1), the decrease of $\tau_o(\text{ICT})$ upon cooling can not be attributed to the energy gap law.

Energy Gap Law and Solvent Polarity. The energy gap law has also been invoked to explain the shortening of the $\tau_o(\text{ICT})$ of CVL as a function of increasing solvent polarity at room temperature.^{2,13,15} $\tilde{\nu}^{\text{max}}(\text{ICT})$ decreases when the polarity becomes larger: 18210 cm⁻¹ (acetone, $\epsilon^{25} = 20.6$), 17990 cm⁻¹ (PrCN, $\epsilon^{25} = 24.2$), 16440 cm⁻¹ (MeCN, $\epsilon^{25} = 36.7$), 16640 cm⁻¹ (DMSO, $\epsilon^{25} = 46.5$), and 16770 cm⁻¹ (PC, $\epsilon^{25} = 64.9$). The lifetimes $\tau_o(\text{ICT})$ ($\leq \tau_i$) of CVL in the solvents with the smallest $\tilde{\nu}^{\text{max}}(\text{ICT})$, PC (0.59 ns), DMSO (0.70 ns) and MeCN (1.2 ns), are clearly shorter than those in PrCN (4.3 ns) and acetone (3.4 ns), see Table S3 in Supporting Information (ref 13) and Table 3. This difference is therefore likewise assumed to originate from an enhanced nonradiative ICT $\rightarrow S_0$ transition, caused by the decrease of the energy difference $\tilde{\nu}^{\text{max}}(\text{ICT})$ between the ICT and its $S_0(\text{FC})$ state, the energy gap law, due to

exponentially increasing FC factors.^{2,13} The same explanation had also been adopted in the case of MGL in polar solvents, from BAC to MeCN.¹⁵

Also for 2,3,5,6-tetrafluoro-4-(dimethylamino)benzonitrile (DMABN4F), 2,3,5,6-tetrafluoro-4-(diethylamino)benzonitrile (DEABN4F), and 2,3,5,6-tetrafluoro-4-(azetidiny)benzonitrile (AZABN4F), $\tau_o(\text{ICT})$ becomes smaller when going from the nonpolar *n*-hexane ($\epsilon^{25} = 1.88$) to the strongly polar MeCN ($\epsilon^{25} = 36.7$), leading to a decrease in the energy gap between the ICT and $S_0(\text{FC})$.⁵¹ For DMABN4F at 25 °C, with $\tilde{\nu}^{\text{max}}(\text{ICT})$ decreasing from 20860 cm⁻¹ (*n*-hexane) to 17300 cm⁻¹ (MeCN), $\tau_o(\text{ICT})$: 0.27 to 0.15 ns (Table S6). Similarly, for DEABN4F $\tilde{\nu}^{\text{max}}(\text{ICT})$ decreases from 21000 to 17900 cm⁻¹ and $\tau_o(\text{ICT})$ drops from 1.5 to 0.54 ns (Tables 6 and S6), whereas $\tilde{\nu}^{\text{max}}(\text{ICT})$ of AZABN4F goes from 21990 to 181900 cm⁻¹ and $\tau_o(\text{ICT})$ from 0.078 to 0.050 ns (Table S6).

Temperature Dependence of $\tau_o(\text{ICT})$ in Other D/A Systems. In our earlier studies of D/A systems, we have encountered two other examples for which $\tau_o(\text{ICT})$ becomes larger with increasing temperature (Table 5): DMABN in MeCN⁴⁴ and 3,4-dicyano-(*N*-methyl-*N*-isopropyl)aniline (34DCMIA) in MeCN.⁶⁴ For both systems, $\tilde{\nu}^{\text{max}}(\text{ICT})$ is rather small, below 20500 cm⁻¹ at 25 °C: 20250 cm⁻¹ (DMABN) and 17280 cm⁻¹ (34DCMIA), see Table 5, similar to CVL in MeCN with $\tilde{\nu}^{\text{max}}(\text{ICT}) = 16440$ cm⁻¹ (Table 1).

With more D/A molecules, in contrast, $\tau_o(\text{ICT})$ becomes shorter with increasing temperature (Table 5). For these systems, $\tilde{\nu}^{\text{max}}(\text{ICT})$ is larger than 21000 cm⁻¹: DMABN, 4-(diethylamino)benzonitrile (DEABN), and 4-(di-*n*-propylamino)benzonitrile (DPrABN) in toluene, as well as with 2,4-dicyano-(*N*-methyl-*N*-isopropyl)aniline (24DCMIA) in DEE,⁶⁴ NTC6 in MeCN,³² *N*-phenylpyrrole (PP) in MeCN,⁴⁸ EtCN,⁴⁸ and PrCN,^{35,36} fluorazene (FPP) in EtCN,^{56,70} and also 4-cyano-*N*-phenylpyrrole (PP4CN) and FPP4CN in MeCN, see Table 5 and Tables S2, S4-S6 in Supporting Information. For this series of D/A systems, $\tilde{\nu}^{\text{max}}(\text{ICT})$ is larger than for CVL, DMABN, and 34DCMIA in MeCN: from 21160 cm⁻¹ for 24DCMIA in DEE at 25 °C to 28150 cm⁻¹ for PP in PrCN at -50 °C. It therefore follows that for sufficiently large gaps between the energies of the ICT state $E(\text{ICT})$ and its corresponding FC state, equal to the ICT fluorescence maximum $\tilde{\nu}^{\text{max}}(\text{ICT})$, $\tau_o(\text{ICT})$ becomes shorter upon heating.

Table 5. Data for CVL and Other D/A Molecules in a Series of Solvents at Different Temperatures

D/A system ^a	ref	Solvent	T (°C)	$\tau_o(\text{ICT})$ (ns)	$\tilde{\nu}^{\text{max}}(\text{ICT})$ (cm ⁻¹)	$\Phi(\text{ISC})$	$\Phi(\text{IC})$
CVL	Tables 1 and 5	MeCN	75	1.45	16970		
			25	1.15	16440	1.0	0.0
			-45	0.84	15840		
DMABN	44	MeCN	75	3.92	20970		
	44		25	3.80	20250	0.80	0.17
	44,70		-45	3.53	19220		
DMABN	67	Toluene	20	2.7	24420 ^b		
	67		-20	3.1			
	48		-45	3.48			
DEABN	67	Toluene	20	2.5	24560 ^b		
	67		-20	2.9			
DPrABN	67	Toluene	20	2.7	24750 ^b		
	67		-20	2.8			
	48		-45	2.90			
24DCMIA	64	MeCN	25		19430	0.83	0.15
24DCMIA	64	DEE ^c	25	4.73	21610		
	64		-45	5.72			
	64		-115	5.42			
34DCMIA	64	MeCN	25	1.17	17280	0.22	0.77
	64		-45	0.85			
NTC6	31	MeCN	75	9.9	23540		
	30,31		25	10.4	23130	0.31	0.09
	31		-45	10.7	22600		
PP	48,70	MeCN	25	4.02	28040	0.74	0.16
	48	MeCN	-20	5.10	27700		
	48,56,70		-45	5.46	27410/27530		
PP	48,56,70	EtCN	-45	4.87	27960/28030		
	48		-90	5.81	27430		
PP	35	PrCN	-50	4.25	28150		
	35		-70	4.90	27940		
FPP	70	MeCN	25		26540	0.65	0.20
FPP	70	EtCN	-45	12.2	26610		
	70		-55	13.3	26510		
	70		-65	13.7	26410		
	70		-75	14.5	26310		
PP4CN	29	MeCN	25	13.6	20750	0.63	0.31
	29		-45	16.7	20080		
FPP4CN	29	MeCN	25	29.7	21550	0.44	0.31
	29		-45	39.2	21040		
DEABN4F	51	<i>n</i> -hexane	25	1.5	21000	0.42	0.57
	51	MeCN	25	0.54	17900	0.09	0.91

^aDMABN: 4-(dimethylamino)benzonitrile; DEABN: 4-(diethylamino)benzonitrile; DPrABN: 4-(di-*n*-propylamino)benzonitrile; MDB: 4-dimethylamino-2,6-dimethyl-benzonitrile; EDB: 4-diethylamino-2,6-dimethyl-benzonitrile; PrDB: 4-di-*n*-propylamino-2,6-dimethyl-benzonitrile; 24DCMIA: 2,4-dicyano-(*N*-methyl-*N*-isopropyl)aniline; 34DCMIA: 3,4-dicyano-(*N*-methyl-*N*-isopropyl)aniline; NTC6: 1-*tert*-butyl-6-cyano-1,2,3,4-tetrahydroquinoline; PP: *N*-phenylpyrrole; FPP: fluorazene; PP4CN: 4-cyano-*N*-phenylpyrrole; FPP4CN: 4-cyanofluorazene; DEABN4F: 2,3,5,6-tetrafluoro-4-(diethylamino)benzonitrile. ^bAt 25 °C. ^cDEE: diethyl ether.

Free Enthalpy Differences ΔG and ΔG^\ddagger . The free enthalpy differences $\Delta G = -RT\ln(k_a/k_d)$ for CVL in MeCN are listed in Table 4. At 25 °C, $\Delta G = -8.9$ kJ/mol, which compares well with the $\Delta G = -9.8$ kJ/mol reported in ref 13, but is rather different from the -3.3 kJ/mol estimated in ref 24 and the previous ΔG of -57 kJ/mol in ref 2. In Table 4, ΔG changes from -6.9 kJ/mol at 75 °C to -10.7 kJ/mol at -45 °C, when taking the data determined directly from τ_2 , τ_1 and A_{12}/A_{11} . By using the corrected data for ΔG based on E_a , E_d , k_a° and k_d° (Table 6, below), the following values are obtained: -7.2 kJ/mol at 75 °C to -11.5 kJ/mol at -45 °C (Table 4). This increase of ΔG is caused by the solvent polarity becoming larger, from $\epsilon = 30.3$ at 75 °C to $\epsilon = 50.2$ at -45 °C.⁸¹

The free energy of activation ΔG_a^\ddagger of CVL in MeCN at 25 °C is 10.1 kJ/mol (Table 4), similar to the ΔG_a^\ddagger of 10.8 kJ/mol that can be calculated from $k_a = 1.23 \times 10^{11} \text{ s}^{-1}$ (Tables 5 and S3) of ref 13. The ΔG_a^\ddagger in Table 4 ranges between 12.0 kJ/mol (or 11.6 kJ/mol corrected) at 75 °C and 8.2 kJ/mol at -45 °C. In the literature, $\Delta G_a^\ddagger = 85.8$ kJ/mol in MeCN has been determined from MD simulation.³⁸ This outcome is much larger than our 10.1 kJ/mol, which must mean that the simulation leads to results far removed from the experimental situation.⁸⁶

Literature Data from Fluorescence Decays and $\Phi'(\text{ICT})/\Phi(\text{LE})$. Instead of using as input data τ_2 , τ_1 , and A_{12}/A_{11} , with $\tau_0 = 39$ ns, such as here, a somewhat different procedure is followed in ref 13. There, τ_2 , τ_1 , and A_{12}/A_{11} are employed, with the condition that $A_{12}/A_{11} = k_a/k_d$. The ratio k_a/k_d is also extracted from $\Phi'(\text{ICT})/\Phi(\text{LE})$, making the assumption that the ratios of the LE and ICT radiative rate constants $k'_f(\text{ICT})/k_f(\text{LE})$ (eq 4) in different solvents depend only on emission frequencies, due to the relation $k_f \propto \nu^3$. $\Delta G = -RT\ln(k_a/k_d)$ is then determined as a weighted average of these two estimates. This approximate solution is only valid, however, when $k_d \gg 1/\tau_o(\text{ICT})$, the high-temperature limit (HTL), leading to the expression $\Phi'(\text{ICT})/\Phi(\text{LE}) = k'_f(\text{ICT})/k_f(\text{LE}) k_a/k_d$ (eq 5 in the present text).^{35,36,87} The condition $k_d \gg 1/\tau_o(\text{ICT})$ is not fulfilled for CVL in PC and DMSO (Table S3) and is barely valid for CVL in acetone and MeCN at 25 °C.⁸⁷ This may jeopardize at least some of the results for k_a and ΔG in ref 13. It also becomes evident from inspection of the Stevens-Ban plots in Figure 6 in ref 13 that the HTL limit applies for CVL in PrCN (butyronitrile, not BuCN) only above -15 °C and in PC for temperatures clearly above 100 °C. Under HTL conditions, $\tau_o(\text{ICT})$ is in fact equal to τ_1 (= 1.2 ns), as seen from the analysis above giving $\tau_o(\text{ICT}) = 1.18$ ns.⁸⁷

ICT Reaction is Not Controlled by Solvent Relaxation Dynamics. The ICT reaction time $1/k_a = 9.4$ ps ($\tau_2 = 9.2$ ps) of the LE \rightarrow ICT reaction of CVL in MeCN at 25 °C is substantially

longer than the mean solvent relaxation time $\langle \tau_{sr} \rangle = 260$ fs, with times of 89 and 630 fs.^{26,27} This means that the ICT reaction of CVL in MeCN is much slower than the solvent relaxation and is hence not solvent controlled, contrary to previous reports in the literature.^{2,13} A similar situation is encountered with DMABN⁴⁴ and PP⁴⁸ in MeCN, different from PP in PrCN at low temperatures,³⁴ for which slow dielectric solvent relaxation interferes with the ICT reaction dynamics below -70 °C.

The conclusion was reached that the ICT reaction of CVL, in conventional solvents²⁴ as well as in ILs,^{13,14} is controlled by solvation dynamics, although it was stated in ref 14 that ‘the distinction between control by solvation dynamics as opposed to other frictional effects could not be definitely established for CVL’. Also Samanta et al. suggested that the LE \rightarrow ICT reaction of CVL in the IL [bmim][Tf₂N] is controlled by solvation dynamics,³⁷ which was questioned in ref 13 (footnote 26).

Activation Energies E_a and E_d . Thermodynamic Data $\Delta H (= E_a - E_d)$. An Arrhenius plot of k_a , k_d , and $1/\tau_o(\text{ICT})$ of CVL in MeCN is shown in Figure 9. The data points for k_d fall on a straight line from 75 down to -25 °C, whereas those for k_a start to deviate from linearity for temperatures above 50 °C. This deviation is caused by the reduction of the contribution of the short time τ_2 to the overall LE fluorescence decay: $A_{12}\tau_2/(A_{12}\tau_2 + A_{11}\tau_1)$, see eq 7. This percentage is equal to 0.83 at -45 °C and 0.22 at 25 °C, but decreases to 0.05 at 75 °C (Figures 5 and 6), apparently not large enough to make an accurate measurement of τ_2 possible at temperatures above 50 °C. From a similar reasoning it becomes clear on the other hand that the contribution of the long time τ_1 to the overall LE fluorescence decay, $A_{11}\tau_1/(A_{12}\tau_2 + A_{11}\tau_1)$, is relatively small at temperatures below -15 °C (0.78 at 25 °C and only 0.17 at -45 °C), leading to the observed lack in accuracy of k_d below -25 °C.

From the slopes of the lines through the data points of k_a and k_d in Figure 9, the activation energies $E_a = 3.9$ kJ/mol and $E_d = 23.6$ kJ/mol are determined (Table 6). From these data, the ICT reaction enthalpy difference $\Delta H = E_a - E_d = -19.7$ kJ/mol is calculated. The corresponding preexponential factors are: $k_a^o = 4.95 \times 10^{11} \text{ s}^{-1}$ and $k_d^o = 3.68 \times 10^{13} \text{ s}^{-1}$, giving $\Delta S = R \ln(k_a^o/k_d^o) = -35.8 \text{ Jmol}^{-1}\text{K}^{-1}$, see Table 6. With DMABN in MeCN similar results are found (Table 6).⁴⁴ From the photostationary data for CVL in MeCN (Stevens-Ban plot, Figure 5) somewhat different data are calculated: $\Delta H(\text{SB}) = -23.9$ kJ/mol, $E_a(\text{SB}) = 8.7$ kJ/mol, and $E_d(\text{SB}) = 32.6$ kJ/mol (Figure 5). These differences may be caused by the temperature dependence of $k'_f(\text{ICT})/k_f(\text{LE})$ (eq 4).⁴⁴

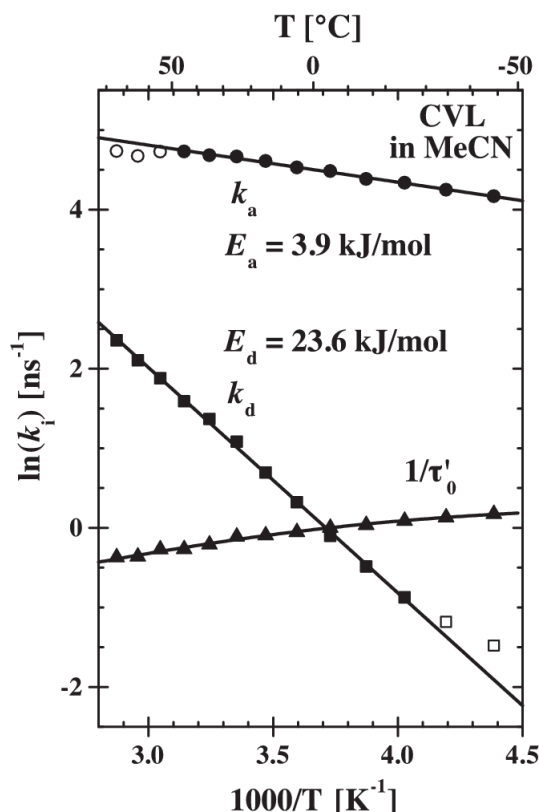


Figure 9. Arrhenius plots of the ICT rate constants k_a (\circ and \bullet) and k_d (\blacksquare and \square) and the reciprocal ICT lifetime $1/\tau'_0(\text{ICT})$ (\blacktriangle), see Scheme 1, of CVL in MeCN. The activation energies $E_a = 3.9$ kJ/mol and $E_d = 23.6$ kJ/mol of k_a and k_d , respectively, are listed in Table 6. The reaction enthalpy $\Delta H = E_a - E_d = -19.7$ kJ/mol. The preexponential factors are: $k_a^0 = 4.95 \times 10^{11} \text{ s}^{-1}$ and $k_d^0 = 3.68 \times 10^{13} \text{ s}^{-1}$. $\Delta S = R \ln(k_a^0/k_d^0) = -35.8 \text{ J mol}^{-1} \text{ K}^{-1}$, see Table 6.

Table 6. Thermodynamic Data and Preexponential Factors for the ICT Reaction of CVL (Figure 9) and DMABN in MeCN

molecule	E_a (kJ/mol) ^a	E_d (kJ/mol) ^b	k_a^0 (10^{11} s^{-1}) ^c	k_d^0 (10^{13} s^{-1}) ^d	ΔH (kJ/mol) ^e	ΔS ($\text{J mol}^{-1} \text{ K}^{-1}$) ^f
CVL	3.9 ± 0.1	23.6 ± 0.3	4.95 ± 0.22	3.68 ± 0.38	-19.7 ± 0.4	-35.8 ± 1.2
DMABN ^g	5.0 ± 0.25	32.0 ± 0.4	18.3 ± 0.2	18.7 ± 0.2	-27.0 ± 0.7	-38.0 ± 1.0

^aActivation energy of the forward LE \rightarrow ICT reaction k_a (Scheme 1). ^bActivation energy of the backward ICT \rightarrow LE reaction k_d (Scheme 1). ^cPreexponential factor of the rate constant k_a . ^dPreexponential factor of the rate constant k_d . ^eEnthalpy difference $\Delta H = E_a - E_d$ of the LE \rightleftharpoons ICT equilibrium. ^fEntropy difference $\Delta S = R \ln(k_a^0/k_d^0)$. ^gData from ref 44.

CVL is a Weakly-Coupled D/A System, Similar to an Exciplex $^1(\text{A}^-\text{D}^+)$. Because of the weak electronic coupling between its D and A moieties, CVL is comparable with 4-(di-*tert*-butylamino)benzonitrile (DTABN), 3-(di-*tert*-butylamino)benzonitrile (mDTABN), and 6-cyanobenzoquinuclidine (CBQ), in which the amino (D) and benzonitrile (A) subgroups are likewise electronically decoupled as a result of their mutually perpendicular configuration, due to the strong steric hindrance of the bulky *tert*-butyl substituents DTABN and the rigidized

molecular structure of CBQ.^{22,45,46} In these weakly coupled D/A systems, the ICT energetics corresponds to that of an intermolecular exciplex, determined by the redox potentials $E(D/D^+)$ and $E(A^-/A)$.^{9,20-22} This is fundamentally different from molecules with strong electronic coupling between D and A, such as DMABN and related aminobenzonitriles, *N*-phenylpyrroles (PP, 4-fluoro-*N*-phenylpyrrole (PP4F), 4-cyano-*N*-phenylpyrrole (PP4CN)), and fluorazenes (FPP, 4-fluorofluorazene (FPP4F), FPP4CN).^{29,30,32,35,44,48,56,61,70}

Conclusion

CVL undergoes a LE \rightarrow ICT reaction in solvents more polar than *n*-hexane ($\epsilon^{25} = 1.88$), such as EAC ($\epsilon^{25} = 5.99$) and THF ($\epsilon^{25} = 7.39$). In these last two solvents and more polar media, the fluorescence spectrum consists of two emission bands, from the LE and the ICT states. The dipole moments of these states are determined from solvatochromic measurements, with $f(\epsilon)$ - $f(n^2)$ as the solvent polarity function for the LE fluorescence maxima $\tilde{\nu}^{\max}$ (LE) and $f(\epsilon)^{-1/2}f(n^2)$ for the ICT emission maxima $\tilde{\nu}^{\max}$ (ICT). The same Onsager radius $\rho = 5.96$ Å is used for LE and ICT, as the size of the cavity to be made in the solvent continuum does not depend on charge distribution in these two states of CVL. The value of ρ is scaled with the dipole moments $\mu_e(\text{LE}) = 10.6$ D and $\mu_e(\text{ICT}) = 17$ D determined for DMABN by TRMC, a method independent of ρ . Employing this approach, $\mu_e(\text{LE}) = 17.4$ D and $\mu_e(\text{ICT}) = 32.7$ D were calculated for CVL. Similar values for the dipole moments were obtained by plotting the emission maxima of CVL versus those of DMABN (LE) and DIABN (ICT), resulting in $\mu_e(\text{LE}) = 16.6$ D and $\mu_e(\text{ICT}) = 34.3$ D. Both dipole moments are considerably larger than those published previously: 10.7 or 9-12 D for $\mu_e(\text{LE})$ and 25 or 24 D for $\mu_e(\text{ICT})$. This discrepancy comes from differences in the fluorescence spectra due to fluorimeter calibration, as well as in the subtraction procedure used to obtain the separate LE and ICT emission spectra. In the case of $\mu_e(\text{LE})$, the different ρ also plays an important role.

The LE and ICT picosecond fluorescence decays of CVL in MeCN between -45 and 75 °C are double exponential. The amplitude ratio A_{21}/A_{22} of the ICT decay is equal to -1, which means that the ICT is not prepared by direct excitation of CVL in the ground state, but is exclusively formed from LE as the precursor. Upon heating from -45 and 75 °C, the decay time τ_2 becomes shorter, from 15.5 to 8.1 ps and τ_1 becomes longer, from 0.84 to 1.58 ns (τ_1), whereas the amplitude ratio A_{12}/A_{11} decreases from 273 to 10.7. An analysis of the times τ_1 , τ_2 , the LE lifetime $\tau_0(\text{LE})$, and the ratio A_{12}/A_{11} as a function of temperature, leads to the ICT activation energies $E_a = 3.9$ kJ/mol and $E_d = 23.6$ kJ/mol, giving $\Delta H = E_a - E_d = -19.7$ kJ/mol. These

results show that the ICT reaction is an activated process. The reaction free enthalpy change ΔG ranges from -10.7 (-11.5) kJ/mol at -45 °C to -6.9 (-7.2) kJ/mol at 75 °C, whereas ΔG^\ddagger changes from 8.2 to 12.0 (11.6) kJ/mol between these temperatures. From the temperature dependence of the fluorescence quantum yield ratio $\Phi'(\text{ICT})/\Phi(\text{LE})$ of CVL in MeCN, a Stevens-Ban (SB) plot, $E_a(\text{SB}) = 8.7$ kJ/mol and $E_d(\text{SB}) = 32.6$ kJ/mol were determined, giving $\Delta H(\text{SB}) = -23.9$ kJ/mol. A possible reason for the difference of these values with those derived from the analysis of the time-resolved fluorescence experiments is the temperature dependence of $k'_f(\text{ICT})/k_f(\text{LE})$, considered to be constant in the SB approach.

The rate constant k_a of the $\text{LE} \rightarrow \text{ICT}$ reaction of CVL in MeCN at 25 °C equals $1.06 \times 10^{11} \text{ s}^{-1}$, equivalent with an ICT reaction time $1/k_a$ of 9.4 ps. This indicates that the reaction is substantially slower than the solvent relaxation in MeCN, which takes place in a mean time of 260 fs. We therefore conclude that the ICT reaction of CVL in MeCN is not solvent controlled, contrary to previous reports in the literature. Our conclusion that there is no solvent control of the ICT reaction is supported by the observation that the LE and ICT fluorescence decays of CVL in MeCN are perfectly double exponential over the entire temperature range from -45 to 75 °C. In the investigation of *N*-phenylpyrrole (PP) in EtCN and PrCN, it was found that such decays can no longer be fitted with two exponentials when solvent dynamics control starts to become dominant, such as with PP in PrCN below -70 °C.

Because of the weak electronic coupling between its D and A moieties, CVL is not comparable with D/A molecules such as DMABN, but much more with DTABN, mDTABN, and CBQ, in which the amino (D) and benzonitrile (A) subgroups are likewise electronically decoupled due to their mutually perpendicular configuration, caused by the strong steric hindrance of the bulky *tert*-butyl substituents DTABN and the rigidized molecular structure of CBQ. In these weakly coupled D/A systems as well as in CVL, the ICT energetics corresponds to that of an intermolecular exciplex $^1(\text{A}^-\text{D}^+)$, determined by the redox potentials of D and A.

Acknowledgement

We thank Jurek Karpiuk (Warsaw) for providing us with pure CVL and for important discussions on its photophysics.

References

Corresponding authors. Fax: +49-551-201-1501, E-mail: (K.A.Z.) kzachar@gwdg.de; (S.I.D.) sdruzhi@gwdg.de; (A.D.) demeter.attila@ttk.mta.hu.

(1) Theocharis, C. R.; Jones, W. Crystal Structure of 3,3-(*p*-*N,N*-dimethylaminophenyl)-6-*N,N*-

dimethylaminophthalide (Crystal-Violet Lactone). *J. Crystal. Spectrosc. Res.* **1984**, *14*, 121-128.

(2) Karpiuk, J. Dual Fluorescence from Two Polar Excited States in One Molecule. Structurally Additive Photophysics of Crystal Violet Lactone. *J. Phys. Chem. A* **2004**, *108*, 11183-11195.

(3) Boese, R.; Weiss, H.-Ch.; Bläser, D. The Melting Point Alternation in Short-Chain *n*-Alkanes: Single Crystal X-Ray Analysis of Propane at 30 K and of *n*-Butane to *n*-Nonane at 90 K. *Angew. Chem. Int. Ed.* **1999**, *38*, 988-992.

(4) White, M. A. The Chemistry Behind Carbonless Copy Paper. *J. Chem. Educ.* **1998**, *75*, 1119-1120.

(5) Kaneko, Y.; Neckers, D. C. Simultaneous Photoinduced Color Formation and Photoinitiated Polymerization. *J. Phys. Chem. A* **1998**, *102*, 5356-5363.

(6) Note that in the present investigation an additional ICT band is found already with CVL in ethyl acetate (EAC, $\epsilon^{25} = 5.99$) as well as in tetrahydrofuran (THF, $\epsilon^{25} = 7.39$), see text, Tables 1 and 2, and Figures S1 and S2 in Supporting Information.

(7) Our definition of the term 'LE state'. When an electron donor(D)/acceptor(A) molecule only emits a single fluorescence band, this is called a LE fluorescence, irrespective of the dipole moment $\mu_e(\text{LE})$ of this state. In such a case, we say that an ICT reaction does not take place. We do speak of an ICT reaction only when a new excited ICT state is produced from the relaxed initially excited $S_1(\text{LE})$ state as the precursor. For this ICT state the condition $\mu_e(\text{ICT}) > \mu_e(\text{LE})$ generally holds, such as for 4-(dimethylamino)benzonitrile (DMABN) in polar solvents with dipole moments of ~17 D (ICT) and ~9 D (LE) (ref 8). A detailed discussion of the limits of the LE nomenclature is presented in ref 9.

(8) Schuddeboom, W.; Jonker, S. A.; Warman, J. M.; Leinhos, U.; Kühnle, W.; Zachariasse, K. A. Excited-State Dipole Moments of Dual Fluorescent 4-(Dialkylamino)benzonitriles: Influence of Alkyl Chain Length and Effective Solvent Polarity. *J. Phys. Chem.* **1992**, *96*, 10809-10819.

(9) Zachariasse, K. A.; Druzhinin, S. I.; Galievsky, V. A.; Kovalenko, S.; Senyushkina, T. A.; Mayer, P.; Noltemeyer, M.; Boggio-Pasqua, M.; Robb, M. A. Counterintuitive Absence of an Excited-State Intramolecular Charge Transfer Reaction with 2,4,6-Tricyanoanilines. Experimental and Computational Results. *J. Phys. Chem. A* **2009**, *113*, 2693-2710.

(10) In refs 2, as well as in refs 19 and 24 (below), a different nomenclature is used, ${}^1\text{CT}_\text{A}$ for LE and ${}^1\text{CT}_\text{B}$ for ICT, to emphasize the large dipole moments of CVL in both states: $\mu({}^1\text{CT}_\text{A}) = 10.7$ D and $\mu({}^1\text{CT}_\text{B}) = 25.2$ D. Similar terms CT_A and CT_B appear in ref 37 (below).

- (11) Jin, H.; Li, X.; Maroncelli, M. Heterogeneous Solute Dynamics in Room Temperature Ionic Liquids. *J. Phys. Chem. B* **2007**, *111*, 13473-13478.
- (12) Jin, H.; Li, X.; Maroncelli, M. Erratum. *J. Phys. Chem. B* **2010**, *114*, 11370.
- (13) Li, X.; Maroncelli, M. Solvent-Controlled Electron Transfer in Crystal Violet Lactone. *J. Phys. Chem. A* **2011**, *115*, 3746-3754.
- (14) Li, X.; Liang, M.; Chakraborty, A.; Kondo, M.; Maroncelli, M. Solvent-Controlled Intramolecular Electron Transfer in Ionic Liquids. *J. Phys. Chem. B* **2011**, *115*, 6592-6607.
- (15) Karpiuk, J. Photoinduced Electron Transfer in Malachite Green Lactone. *Phys. Chem. Chem. Phys.* **2003**, *5*, 1078-1090.
- (16) Bizjak, T.; Karpiuk, J.; Lochbrunner, S.; Riedle, E. 50-fs Photoinduced Intramolecular Charge Separation in Triphenylmethane Lactones. *J. Phys. Chem. A* **2004**, *108*, 10763-10769.
- (17) Karpiuk, J.; Svartsov, Y.N.; Nowacki, J. Photoinduced Intramolecular Charge Transfer to *Meta* Position of Benzene Ring in 6-Aminophthalides. *Phys. Chem. Chem. Phys.* **2005**, *7*, 4070-4081.
- (18) Karpiuk, J.; Karolak, E.; Nowacki, J. Photoinduced Intramolecular Charge Separation and Recombination in a Donor-Acceptor Dyad Linked *via* Tetrahedral Carbon Atom. Photophysics of a Malachite Green Lactone Analogue. *Pol. J. Chem.* **2008**, *82*, 865-882.
- (19) Karpiuk, J. Tuneable White Fluorescence from Intramolecular Exciplexes. *Phys. Chem. Chem. Phys.* **2010**, *12*, 8804-8809.
- (20) Weller, A. Singlet- and Triplet Exciplexes. In *The Exciplex*; Gordon, M.; Ware, W. R., Eds.; Academic Press: New York, 1975; pp 23-38.
- (21) Weller, A. Photoinduced Electron Transfer in Solution: Exciplex and Radical Ion Pair Formation. Free Enthalpies and Their Solvent Dependence. *Z. Phys. Chem.* **1982**, *133*, 93-98.
- (22) von der Haar, Th.; Hebecker, A.; Il'ichev, Yu. V.; Jiang, Y.-B.; Kühnle, W.; Zachariasse, K. A. Excited-State Intramolecular Charge Transfer in Donor/Acceptor-Substituted Aromatic Hydrocarbons and in Biaryls. The Significance of the Redox Potentials of the D/A Subsystems. *Recl. Trav. Chim. Pays-Bas* **1995**, *114*, 430-442.
- (23) Shida, T. *Electronic Absorption Spectra of Radical Ions*; Elsevier: New York, 1988.
- (24) Schmidhammer, U.; Megerle, U.; Lochbrunner, S.; Riedle, E.; Karpiuk, J. The Key Role of Solvation Dynamics in Intramolecular Electron Transfer: Time-Resolved Photophysics of crystal Violet Lactone. *J. Phys. Chem. A* **2008**, *112*, 8487-8496.

- (25) Druzhinin, S. I.; Galievsky, V. A.; Zachariasse, K. A. Photoproduct Formation with 4-Aminobenzonitriles in Acetonitrile and Its Effect on Photophysical Measurements. *J. Phys. Chem. A* **2005**, *109*, 11213-11223.
- (26) Horng, M. L.; Gardecki, J. A.; Papazyan, A.; Maroncelli, M. Subpicosecond Measurements of Polar Solvation Dynamics: Coumarin 153 Revisited. *J. Phys. Chem.* **1995**, *99*, 17311-17337.
- (27) Pérez Lustres, L.; Rodriguez-Prieto, F.; Mosquera, M.; Senyushkina, T.; Kovalenko, S.A. Ultrafast Proton Transfer to Solvent: Molecularity and Intermediates from Solvation- and Diffusion-Controlled Regimes. *J. Am. Chem. Soc.* **2007**, *129*, 5408-5418.
- (28) Agmon, N. Dynamic Stokes Shift in Coumarin: Is it Only Relaxation? *J. Phys. Chem.* **1990**, *94*, 2959-2963.
- (29) Druzhinin, S. I.; Kovalenko, S. A.; Senyushkina, T. A.; Demeter, A.; Machinek, R.; Noltemeyer, M.; Zachariasse, K. A. Intramolecular Charge Transfer with the Planarized 4-Cyanofluorazene and its Flexible Counterpart 4-Cyano-*N*-phenylpyrrole. Picosecond Fluorescence Decays and Femtosecond Excited-State Absorption. *J. Phys. Chem. A* **2008**, *112*, 8238-8253. Erratum: *J. Phys. Chem. A* **2009**, *113*, 520.
- (30) Zachariasse, K. A.; Druzhinin, S. I.; Bosch, W.; Machinek, R. Intramolecular Charge Transfer with the Planarized 4-Aminobenzonitrile 1-*tert*-Butyl-6-cyano-1,2,3,4-tetrahydroquinoline (NTC6). *J. Am. Chem. Soc.* **2004**, *126*, 1705-1715.
- (31) Druzhinin, S. I.; Kovalenko, S. A.; Senyushkina, T.; Zachariasse, K. A. Dynamics of Ultrafast Intramolecular Charge Transfer with 1-*tert*-Butyl-6-cyano-1,2,3,4-tetrahydroquinoline (NTC6) in *n*-Hexane and Acetonitrile. *J. Phys. Chem. A* **2007**, *111*, 12878-12890.
- (32) Druzhinin, S. I.; Mayer, P.; Stalke, D.; von Bülow, R.; Noltemeyer, M.; Zachariasse, K. A. Intramolecular Charge Transfer with 1-*tert*-Butyl-6-cyano-1,2,3,4-tetrahydroquinoline (NTC6) and Other Aminobenzonitriles. A Comparison of Experimental Vapor Phase Spectra and Crystal Structures with Calculations. *J. Am. Chem. Soc.* **2010**, *132*, 7730-7744.
- (33) For CVL the energy differences between the LE fluorescence maximum in *n*-hexane and the LE and ICT emission maxima in a series of solvents, $\{\tilde{\nu}^{\max}(\text{LE}, n\text{-hexane}) - \tilde{\nu}^{\max}(\text{LE})\}$ and $\{\tilde{\nu}^{\max}(\text{LE}, n\text{-hexane}) - \tilde{\nu}^{\max}(\text{ICT})\}$ are employed in the solvatochromic analysis in ref 13, using a spherical-polarizable-dipole solute, dielectric continuum solvent model. In this analysis, different Onsager cavity radii ρ are used for the LE and ICT states of CVL, with the values $\rho(\text{LE}) = 3.6 \text{ \AA}$ and $\rho(\text{ICT}) = 5.8 \text{ \AA}$, taken from ref 2. Although this solvatochromic analysis is different from that in ref 2, similar dipole moments are obtained: $\mu_e(\text{LE}) = 9\text{-}12 \text{ D}$

and $\mu_e(\text{ICT}) = 24$ D, as compared with 11 and 25 D from ref 2. Note that $\tilde{\nu}^{\text{max}}(\text{ICT})$ and $\tilde{\nu}^{\text{max}}(\text{LE})$ are both plotted in ref 2 against $f^{-1/2}f'$, different from the approach adopted here, in which $\tilde{\nu}^{\text{max}}(\text{LE})$ is plotted vs $f \cdot f'$, see text.

(34) The method employed in ref 13, is only strictly valid under conditions where the rate constant k_d of the thermal back reaction $\text{ICT} \rightarrow \text{LE}$ is much larger than the reciprocal lifetime $\tau_o(\text{ICT})$. This limiting situation $k_d \gg 1/\tau_o(\text{ICT})$ has been called the high-temperature limit (HTL). See text and ref 65, below.

(35) Druzhinin, S. I.; Galievsky, V. A.; Yoshihara, T.; Zachariasse, K. A. Intramolecular Charge Transfer and Dielectric Solvent Relaxation in *n*-Propyl Cyanide. *N*-Phenylpyrrole and 4-Dimethylamino-4'-cyanostilbene. *J. Phys. Chem. A* **2006**, *110*, 12760-12768.

(36) With *N*-phenylpyrrole (PP) in PrCN below -70 °C (ref 35), a deviation from double-exponential character of the LE and ICT fluorescence decays is observed, caused by interference of dielectric solvent relaxation with the ICT reaction, both taking place at a comparable time range.

(37) Santosh, K.; Samanta, A. Modulation of the Excited State Intramolecular Electron Transfer Reaction and Dual Fluorescence of Crystal Violet Lactone in Room Temperature Ionic Liquids. *J. Phys. Chem. B* **2010**, *114*, 9195-9200.

(38) Anapureddy, H. V. R.; Margulis, C. J. Controlling the Outcome of Electron Transfer in Ionic Liquids. *J. Phys. Chem. B* **2009**, *113*, 12005-12012.

(39) Demchenko, A. P. The Red-Edge Effects: 30 Years of Exploration. *Luminescence* **2002**, *17*, 19-42.

(40) Mandal, P. K.; Sarkar, M.; Samanta, A. Excitation-Wavelength-Dependent Fluorescence Behavior of Some Dipolar Molecules in Room Temperature Ionic Liquids. *J. Phys. Chem. A* **2004**, *108*, 9048-9053.

(41) Mandal, P. K.; Paul, A.; Samanta, A. Excitation Wavelength Dependent Fluorescence Behavior of the Room Temperature Ionic Liquids and Dissolved Dipolar Solutes. *J. Photochem. Photobiol. A: Chem.* **2006**, *182*, 113-120.

(42) Paul, A.; Mandal, P. K.; Samanta, A. On the Optical Properties of the Imidazolium Ionic Liquids. *J. Phys. Chem. B* **2005**, *109*, 9148-9153.

(43) Samanta, A. Dynamic Stokes Shift and Excitation Wavelength Dependent Fluorescence of Dipolar Molecules in Room Temperature Ionic Liquids. *J. Phys. Chem. B* **2006**, *110*, 13704-13716.

- (44) Druzhinin, S. I.; Ernstring, N. P.; Kovalenko, S. A.; Pérez Lustres, L.; Senyushkina, T.; Zachariasse, K. A. Dynamics of Ultrafast Intramolecular Charge Transfer with 4-(Dimethylamino)benzonitrile. *J. Phys. Chem. A* **2006**, *110*, 2955-2969.
- (45) Druzhinin, S. I.; Dubbaka, S. R.; Knochel, P.; Kovalenko, S. A.; Mayer, P.; Senyushkina, T.; Zachariasse, K. A. Ultrafast Intramolecular Charge Transfer with Strongly Twisted Aminobenzonitriles: 4-(Di-*tert*-butylamino)benzonitrile and 3-(Di-*tert*-butylamino)benzonitrile. *J. Phys. Chem. A* **2008**, *112*, 2749-2761.
- (46) Zachariasse, K. A.; Grobys, M.; von der Haar, Th.; Hebecker, A.; Il'ichev, Yu. V.; Jiang, Y.-B.; Morawski, O.; Kühnle, W. Intramolecular Charge Transfer in the Excited State. Kinetics and Configurational Changes. *J. Photochem. Photobiol. A: Chem.* **1996**, *102*, 59-70. Erratum: *J. Photochem. Photobiol. A: Chem.* **1998**, *115*, 259.
- (47) Zachariasse, K. A.; Druzhinin, S. I.; Galievsky, V. A.; Demeter, A.; Allonas, X.; Kovalenko, S. A.; Senyushkina, T. A. Pentacyano-*N,N*-dimethylaniline in the Excited State. Only Locally Excited State Emission, in Spite of the Large Electron Affinity of the Pentacyanobenzene Subgroup. *J. Phys. Chem. A* **2010**, *114*, 13031-13039.
- (48) Yoshihara, T.; Druzhinin, S. I.; Demeter, A.; Kocher, N.; Stalke, D.; Zachariasse, K. A. Kinetics of Intramolecular Charge Transfer with *N*-Phenylpyrrole in Alkyl Cyanides. *J. Phys. Chem. A* **2005**, *109*, 1497-1509.
- (49) Yoshihara, T.; Galievsky, V. A.; Druzhinin, S. I.; Saha, S.; Zachariasse, K. A. Singlet Excited State Dipole Moments of Dual Fluorescent *N*-Phenylpyrroles and 4-(Dimethylamino)benzonitrile from Solvatochromic and Thermochromic Spectral Shifts. *Photochem. Photobiol. Sci.* **2003**, *2*, 342-353.
- (50) Demas, J. N.; Crosby, G. A. Measurement of Photoluminescence Quantum Yields. Review. *J. Phys. Chem.* **1971**, *75*, 991-1024.
- (51) Galievsky, V. A.; Druzhinin, S. I.; Demeter, A.; Jiang, Y.-B.; Kovalenko, S. A.; Pérez Lustres, L.; Venugopal, K.; Ernstring, N. P.; Allonas, X.; Noltemeyer, M.; Machinek, R.; Zachariasse, K. A. Ultrafast Intramolecular Charge Transfer and Internal Conversion with Tetrafluoro-Aminobenzonitriles. *Chem. Phys. Chem.* **2005**, *6*, 2307-2323.
- (52) Suzuki, K.; Demeter, A.; Kühnle, W.; Tauer, E.; Zachariasse, K. A.; Tobita, S.; Shizuka, H. Internal Conversion in 4-Substituted 1-Naphthylamines. Influence of the Electron Donor/Acceptor Substituent Character. *Phys. Chem. Chem. Phys.* **2000**, *2*, 981-991.
- (53) Demeter, A.; Bérces, T.; Zachariasse, K. A. Dual Fluorescence and Intramolecular Charge Transfer with *N*-Phenylphenanthridinones. *J. Phys. Chem. A* **2001**, *105*, 4611-4621.

- (54) Druzhinin, S. I.; Demeter, A.; Niebuer, M.; Tauer, E.; Zachariasse, K. A. Fast Internal Conversion, Dual Fluorescence and Intramolecular Charge Transfer in 9-Cyano-10-(dimethylamino)anthracene. *Res. Chem. Intermed.* **1999**, *25*, 531-550.
- (55) Demeter, A.; Bérces, T. Study of the Long-Lived Intermediate Formed in the Photoreduction of Benzophenone by Isopropyl Alcohol. *J. Photochem. Photobiol.A: Chem.* **1989**, *46*, 27-40.
- (56) Druzhinin, S. I.; Kovalenko, S. A.; Senyushkina, T. A.; Demeter, A.; Januskevicius, R.; Mayer, P.; Stalke, D.; Machinek, R.; Zachariasse, K. A. Intramolecular Charge Transfer with 4-Fluorofluorazene and the Flexible 4-Fluoro-*N*-phenylpyrrole. *J. Phys. Chem. A* **2009**, *113*, 9304-9320.
- (57) Baumann, W.; Bischof, H.; Brittinger, J.-C.; Rettig, W.; Rotkiewicz, K. Considerations of the Dipole Moment of Molecules Forming the Twisted Intramolecular Charge Transfer State. *J. Photochem. Photobiol. A: Chem.* **1992**, *64*, 49-72.
- (58) Il'ichev, Yu. V.; Kühnle, W.; Zachariasse, K. A. Photophysics of 4-Dimethylamino-4'-cyanostilbene and 4-Azetidinyl-4'-cyanostilbene. Time-Resolved Fluorescence and Trans-Cis Photoisomerisation. *Chem. Phys.* **1996**, *211*, 441-453.
- (59) Suppan, P.; Ghoneim, N. *Solvatochromism*, The Royal Society of Chemistry, Cambridge, UK, 1997.
- (60) Liptay, W. Dipole Moments and Polarizabilities of Molecules in Excited Electronic States. In *Excited States*, Vol. 1; Lim, E. C., Ed.; Academic Press: New York, USA, 1974, pp 129-229.
- (61) Yoshihara, T.; Druzhinin, S. I.; Zachariasse, K. A. Fast Intramolecular Charge Transfer with a Planar Rigidized Electron Donor/Acceptor Molecule. *J. Am. Chem. Soc.* **2004**, *126*, 8535-8539.
- (62) Galievsky, V. A.; Druzhinin, S. I.; Demeter, A.; Mayer, P.; Kovalenko, S. A.; Senyushkina, T. A.; Zachariasse, K. A. Ultrafast Intramolecular Charge Transfer with *N*-(4-cyanophenyl)carbazole. Evidence for a LE Precursor and Dual LE + ICT Fluorescence. *J. Phys. Chem. A* **2010**, *114*, 12622-12638.
- (63) Demeter, A.; Druzhinin, S. I.; Kovalenko, S. A.; Senyushkina, T. A.; Zachariasse, K. A. *J. Phys. Chem. A* **2011**, *115*, 1521-1537.
- (64) Galievsky, V. A.; Druzhinin, S. I.; Demeter, A.; Kovalenko, S. A.; Senyushkina, T. A.; Mayer, P.; Zachariasse, K. A. Presence and Absence of the Excited State Intramolecular Charge Transfer with the Six Isomers of Dicyano-*N,N*-dimethylaniline and Dicyano-(*N*-methyl-*N*-isopropyl)aniline. *J. Phys. Chem. A* **2011**, *115*, 10823-10845.

- (65) Heine, A.; Herbst-Irmer, R.; Stalke, D.; Kühnle, W.; Zachariasse, K. A. Structure and Crystal Packing of 4-Aminobenzonitriles and 4-Amino-3,5-dimethylbenzonitriles. *Acta Cryst.* **1994**, *B50*, 363-373.
- (66) Demeter, A.; Druzhinin, S.; George, M.; Haselbach, E.; Roulin, J.-L.; Zachariasse, K. A. Dual Fluorescence and Fast Intramolecular Charge Transfer with 4-(Diisopropylamino)benzonitrile in Alkane Solvents. *Chem. Phys. Lett.* **2000**, *323*, 351-360.
- (67) Il'ichev, Yu. V.; Kühnle, W.; Zachariasse, K. A. Intramolecular Charge Transfer in Dual Fluorescent 4-(Dialkylamino)benzonitriles. Reaction Efficiency Enhancement by Increasing the Size of the Amino and Benzonitrile Subunits by Alkyl Substituents. *J. Phys. Chem. A* **1998**, *102*, 5670-5680.
- (68) In ref 13, $\Phi'(\text{ICT})/(\Phi'(\text{ICT}) + \Phi(\text{LE})) = 0.93 \pm 0.5$.
- (69) Zachariasse, K.A. Kinetics and Thermodynamics of Excimer Formation. Excited State Equilibria. *Trends Photochem. Photobiol.* **1994**, *3*, 211-227.
- (70) Druzhinin, S. I.; Kovalenko, S. A.; Senyushkina, T. A.; Demeter, A.; Zachariasse, K. A. Intramolecular Charge Transfer with Fluorazene and *N*-Phenylpyrrole. *J. Phys. Chem. A* **2010**, *114*, 1621-1632.
- (71) Striker, G. Effective Implementation of Modulating Functions. In *Deconvolution and Reconvolution of Analytical Signals*; Bouchy, M., Ed.; University Press: Nancy, France, 1982; pp 329-364.
- (72) Leinhos, U.; Kühnle, W.; Zachariasse, K. A. Intramolecular Charge Transfer and Thermal Exciplex Dissociation with *p*-Aminobenzonitriles in Toluene. *J. Phys. Chem.* **1991**, *95*, 2013-2021.
- (73) From $\tau_2 = 9.2$ ps, $\tau_1 = 1180$ ps, $\tau_0(\text{LE}) = 39$ ns and $A = A_{12}/A_{11} = 35.3$: $k_a = 105.7 \times 10^9 \text{ s}^{-1}$ and $k_d = 2.95 \times 10^9 \text{ s}^{-1}$, hence $k_a/k_d = 35.8$, not exactly equal to A . The lifetime $\tau_o(\text{ICT}) = 1.15$ ns.
- (74) The exact value of $\tau_0(\text{LE})$ has hardly any influence on that of k_a and k_d . Also the impact on $\tau_o(\text{ICT})$ is very small. For $\tau_2 = 9.2$ ps, $\tau_1 = 1180$ ps, $A = A_{12}/A_{11} = 35.3$, and $\tau_0(\text{LE}) = 39$ ns (Table 4): $k_a = 105.7 \times 10^9 \text{ s}^{-1}$ and $k_d = 2.95 \times 10^9 \text{ s}^{-1}$ ($k_a/k_d = 35.8$), and $\tau_o(\text{ICT}) = 1.15$ ns. Even with $\tau_0(\text{LE}) = 1$ ns, for example: $k_a = 104.7 \times 10^9 \text{ s}^{-1}$ and $k_d = 2.98 \times 10^9 \text{ s}^{-1}$ ($k_a/k_d = 35.13$), and $\tau_o(\text{ICT}) = 1.19$ ns, practically the same results as with $\tau_0(\text{LE}) = 39$ ns, see Table 4. With $\tau_0(\text{LE}) = 5$ ns: $k_a = 105.5 \times 10^9 \text{ s}^{-1}$ and $k_d = 2.95 \times 10^9 \text{ s}^{-1}$ ($k_a/k_d = 35.76$), and $\tau_o(\text{ICT}) = 1.16$ ns, in fact identical to the results calculated with $\tau_0(\text{LE}) = 39$ ns.
- (75) After correction of τ_2 at high temperatures and of A_{12}/A_{11} at low temperatures, see the

Arrhenius plots in Figure 9 and text, k_a at 75 °C becomes larger ($135 \times 10^9 \text{ s}^{-1}$) and k_d at -45 °C smaller ($0.14 \times 10^9 \text{ s}^{-1}$) (Table 4).

(76) Druzhinin, S. I.; Demeter, A.; Galievsky, V. A.; Yoshihara, T.; Zachariasse, K. A. Thermally Activated Internal Conversion with 4-(Dimethylamino)benzonitrile, 4-(Methylamino)benzonitrile and 4-Aminobenzonitrile in Alkane Solvents. No Correlation with Intramolecular Charge Transfer. *J. Phys. Chem. A* **2003**, *107*, 8075-8085.

(77) Zachariasse, K. A.; Maçanita, A. L.; Kühnle, W. Chain Length Dependence of Intramolecular Excimer Formation with 1,*n*-Bis(1-pyrenecarboxy)alkanes for $n = 1-16, 22$, and 32 . *J. Phys. Chem. B* **1999**, *103*, 9356-9365.

(78) Maçanita, A. L.; Zachariasse, K. A. Viscosity Dependence of Intramolecular Excimer Formation with 1,5-Bis(1-pyrenecarboxy)pentane in Alkane Solvents as a Function of Temperature. *J. Phys. Chem. A* **2011**, *115*, 3183-3195.

(79) Landolt-Börnstein, *Numerical Data and Functional Relationships in Science and Technology, New Series*; Lechner, M. D., Ed.; Group III, Volume 38B, Springer, Berlin, 1996.

(80) Temperature dependence of the refractive index n of MeCN: $n^{-45} = 1.3780$; $n^{25} = 1.3417$; $n^{75} = 1.3169$ (from ref 79).

(81) Landolt-Börnstein, *Numerical Data and Functional Relationships in Science and Technology, New Series*; Madelung, O., Ed.; Group IV, Volume 6, Springer, Berlin, 1991.

(82) Siebrand, W. Radiationless Transitions in Polyatomic Molecules. II. Triplet-Ground-State Transitions in Aromatic Hydrocarbons. *J. Chem. Phys.* **1967**, *47*, 2411-2422.

(83) Englman, R.; Jortner, J. The Energy Gap for Radiationless Transitions in Large Molecules. *Mol. Phys.* **1970**, *18*, 145-164.

(84) Kakitani, T.; Mataga, N. Different Energy Gap Laws for the Three Types of Electron-Transfer Reactions in Polar Solvents. *J. Phys. Chem.* **1986**, *90*, 993-995.

(85) Bixon, M.; Jortner, J.; Cortes, J.; Heitele, H.; Michel-Beyerle, M. E. Energy Gap Law for Nonradiative and Radiative Charge Transfer in Isolated and in Solvated Supramolecules. *J. Phys. Chem.* **1994**, *98*, 7289-7299.

(86) The simulated LE and ICT fluorescence of CVL in MeCN spectra are very different from the experimental spectra (Figure 1b) as is clear from data estimated from Figure 7 in ref 38: $\tilde{\nu}^{\text{max}}$ (LE) = 18900 cm^{-1} (ref 38), 22700 cm^{-1} (Table 2) and $\tilde{\nu}^{\text{max}}$ (ICT) = 9500 cm^{-1} (ref 38), 16400 cm^{-1} (Table 2). The overall fluorescence spectra extend from 3000 to 23000 cm^{-1} in the simulation and from 9000 to 25500 cm^{-1} in Figure 1b. The differences outlined here do not lead to an increase of the credibility of the simulations. Note that the Marcus approach used in ref

38, basically a harmonic approximation, does not contain specific details of the molecular system. It treats the solvent as a dielectric continuum.

(87) From the decay parameters appearing for CVL at 25 °C in Table 3 of ref 13, two solvents (acetone and MeCN) are analyzed here using our approach, i.e., the analysis of τ_2 , τ_1 , and A_{12}/A_{11} , with $\tau_0 = 39$ ns (see text). Acetone: case (1): $\tau_2 = 22$ ps, $\tau_1 = 3.6$ ns, $A_{12}/A_{11} = 0.92/0.08 = 11.50$ (not optimal double exponential decay, Figure 7 in ref 13). With $\tau_0 = 39$ ns from ref 16: $k_a = 4.18 \times 10^{10} \text{ s}^{-1}$, $k_d = 3.59 \times 10^9 \text{ s}^{-1}$, $\tau_o(\text{ICT}) = 3.34$ ns, $1/\tau_o(\text{ICT}) = 0.30 \times 10^9 \text{ s}^{-1}$. From these results, $K_{\text{eq}} = k_a/k_d = 11.64$ ($\sim A_{12}/A_{11}$ 11.50) and $\Delta G = -RT\ln(k_a/k_d) = -6.08$ kJ/mol. Acetone, case (2): Employing $\tau_1 = 2.6$ ns (from Figure 7 in ref 13) practically identical results are obtained for k_a and k_d , but not for $\tau_o(\text{ICT})$, which is roughly equal to τ_1 (see text): $k_a = 4.18 \times 10^{10} \text{ s}^{-1}$, $k_d = 3.58 \times 10^9 \text{ s}^{-1}$, $\tau_o(\text{ICT}) = 2.41$ ns, $1/\tau_o(\text{ICT}) = 0.41 \times 10^9 \text{ s}^{-1}$. Hence, $K_{\text{eq}} = k_a/k_d = 11.70$ and $\Delta G = -6.10$ kJ/mol. Acetone, case (3): From the 3-exp decays (Figure 7, ref 13) with $\tau_2 = 20$ ps, $\tau_1 = 2.8$ ns, $A_{12}/A_{11} = 0.91/0.07 = 13.0$, neglecting an impurity decay time of 200 ps: $k_a = 4.64 \times 10^{10} \text{ s}^{-1}$, $k_d = 3.52 \times 10^9 \text{ s}^{-1}$, $\tau_o(\text{ICT}) = 2.62$ ns, $1/\tau_o(\text{ICT}) = 0.38 \times 10^9 \text{ s}^{-1}$. From which results, $K_{\text{eq}} = k_a/k_d = 13.18$, $\Delta G = -6.39$ kJ/mol. For the above cases (1) to (3), the condition $k_d \gg 1/\tau_o(\text{ICT})$ and our eq 5 are valid. In Table 3 (ref 13), with $\ln(A_{12}/A_{11})$ as a weighted average from fluorescence decays and emission spectra, the following data appear: $\Delta G = -6.8$ kJ/mol and $k_a = 4.2 \times 10^{10} \text{ s}^{-1}$, as compared with $\Delta G = -6.1$ kJ/mol and $k_a = 4.2 \times 10^{10} \text{ s}^{-1}$, calculated from the data (1) via our method, as described above. For MeCN (Table 3, ref 13): $\tau_2 = 8$ ps, $\tau_1 = 1.2$ ns, $A_{12}/A_{11} = 0.98/0.02 = 49.00$. With our $\tau_0 = 39$ ns: $k_a = 1.23 \times 10^{11} \text{ s}^{-1}$, $k_d = 2.47 \times 10^9 \text{ s}^{-1}$, $\tau_o(\text{ICT}) = 1.18$ ns, $1/\tau_o(\text{ICT}) = 0.85 \times 10^9 \text{ s}^{-1}$. $K_{\text{eq}} = k_a/k_d = 49.7$, $\Delta G = -9.68$ kJ/mol. In Table 3 (ref 13), the following results appear: $\Delta G = -9.8$ kJ/mol and $k_a = 1.20 \times 10^{11} \text{ s}^{-1}$, the same results, $\Delta G = -9.7$ kJ/mol and $k_a = 1.23 \times 10^{10} \text{ s}^{-1}$, calculated via our procedure. In MeCN at 25 °C, the condition $k_d \gg 1/\tau_o(\text{ICT})$ is marginally valid, see our Figure 5.

For Table of Contents Only:

τ_i [ps]	9.2	1180	χ^2
$A_{1i}(\text{LE})$	5.3	0.15	0.93
$A_{2i}(\text{ICT})$	-1.64	1.64	0.90

